Chapter 3
Prediction of Nonlinear Forced Response on Ancillary Subsystem Components Attached to Reduced Linear Systems

Sergio E. Obando, Peter Avitabile, and Jason Foley

Abstract Industrial size FE models often times involve multiple interconnected linear components with very high fidelity resolution and very refined mesh. The prediction of the dynamic characteristics of this type of system can be costly and inefficient, in particular, when localized nonlinearities are present due to coupling elements such as hard contacts, isolation mounts, gap springs, bilinear springs, etc. Reduction methodologies are currently employed in this setting to decrease the set of active degrees of freedom in the FEM and efficiently compute the nonlinear system response. For complete multi-component systems with complicated nonlinear subcomponent configurations, the dynamic response of the system will have the embedded characteristics of the appended/ancillary subcomponents but the fidelity of the model will be highly dependent on the quality and resolution of the model. Therefore, sufficient substructure information is needed for an accurate prediction of the response of the appendage and/or its coupling structure.

In this work, analytical models of a multi-component beam system with nonlinear contact interactions were created to investigate the prediction of the dynamic response of ancillary subsystem components. The ancillary structure will be assumed to be dynamically active but will not contain any degrees of freedom in the reduced model. The models will be created first at full space as a reference and then reduction techniques will be used to determine the necessary information in order to accurately predict the displacement at the appendage. The dynamic characteristics of the ancillary component will be extracted using the subcomponent information available from the system. The solution is obtained from piecewise linear approximations of the reduced order model and expansion is used to obtained system level response at all DOF.

Keywords Forced nonlinear response • Reduced order modeling • Cascaded components

Nomenclature

Symbols

$\{X_n\}$	Full Set Displacement Vector
$\{X_a\}$	Reduced Set Displacement Vector
$\{X_d\}$	Deleted Set Displacement Vector
$[M_a]$	Reduced Mass Matrix
$[M_n]$	Expanded Mass Matrix
$[K_a]$	Reduced Stiffness Matrix
$[K_n]$	Expanded Stiffness Matrix
$[U_a]$	Reduced Set Shape Matrix
$[U_n]$	Full Set Shape Matrix
$[U_a]^g$	Generalized Inverse
$[T]$	Transformation Matrix
$[T_U]$	SEREP Transformation Matrix

S.E. Obando (✉) • P. Avitabile
Structural Dynamics and Acoustic Systems Laboratory, University of Massachusetts Lowell, One University Avenue, Lowell, MA 01854, USA
e-mail: sergio.e.obando@gmail.com

J. Foley
Air Force Research Laboratory, Munitions Directorate, Fuzes Branch, Eglin Air Force Base, 306 W. Eglin Blvd, Bldg 432, Eglin AFB, Valparaiso, FL 32542-5430, USA

G. Kerschen (ed.), *Nonlinear Dynamics, Volume 1*, Conference Proceedings of the Society for Experimental Mechanics Series, DOI 10.1007/978-3-319-15221-9_3

$\{p\}$	Modal Displacement Vector
$[M]$	Physical Mass Matrix
$[C]$	Physical Damping Matrix
$[K]$	Physical Stiffness Matrix
$\overline{M}$	Diagonal Modal Mass Matrix
$\overline{K}$	Diagonal Modal Stiffness Matrix
$\overline{C}$	Diagonal Modal Damping Matrix
$[\bar{I}]$	Identity Matrix
$\{F\}$	Physical Force Vector
$\{\ddot{x}\}$	Physical Acceleration Vector
$\{\dot{x}\}$	Physical Velocity Vector
$\{x\}$	Physical Displacement Vector
$\overrightarrow{\ddot{x}}_0$	Initial Acceleration Vector
$\overrightarrow{\dot{x}}_0$	Initial Velocity Vector
$\overrightarrow{x}_0$	Initial Displacement Vector
$\overrightarrow{F}_0$	Initial Force Vector
α	Parameter for Newmark Integration
β	Parameter for Newmark Integration
Δt	Time Step

Subscript

1	State 1
2	State 2
12	State 1–2
i	Row i
j	Column j
n	Full Set of Finite Element DOF
a	Reduced Set of DOF
d	Deleted (Omitted) Set of DOF
U	SEREP
TIE	Stiffness Tie Matrix
SYS	System AB of Assembled Components

Superscript

T	Transpose
g	Generalized Inverse
k	kth Degree of Freedom
-1	Standard Inverse
A	Component A
B	Component B

Acronyms

ADOF	Reduced Degrees of Freedom
NDOF	Full Space Degrees of Freedom
DOF	Degrees of Freedom

ERMT Equivalent Reduced Model Technique
FEM Finite Element Model
MAC Modal Assurance Criterion
SEREP System Equivalent Reduction Expansion Process
TRAC Time Response Assurance Criterion

3.1 Introduction

Multi-component structural systems are commonly used in the modeling of dynamic systems. In order to simplify such complex mathematical models, peripheral/ancillary components are often times grouped as larger substructures of the total assembly. While the contribution to the dynamic characteristics of the system from the subsystem ancillary components can seem small, the accuracy of the prediction of the system level response may be compromised if a sufficiently detailed model is not used.

Industrial size FE models of this high resolution carry a large cost and lead to a significant amount of time and computational resources. For instance, the design stage of manufactured goods often times requires analysis of a multitude of configurations and scenarios that cannot be quickly evaluated. Moreover, additional challenges occur when already large intricate models involve complicated nonlinear subcomponent configuration and complex connections/coupling elements. A nonlinear solution scheme for these types of models is inefficient considering the localized nature of the nonlinearities or their overall effect at limited times on the full response of the system. In this setting, reduction methodologies are currently employed to efficiently decrease the set of active degrees of freedom (ADOF) down to a more manageable size. In particular, a family of nonlinear problems consisting of linear components interconnected with nonlinear elements allows for efficient reduced modeling and a solution composed of piecewise linear approximations.

The dynamics of this class of nonlinear problems can be accurately captured by observing the changes of state of the linear components with time while implementing efficient reduced order modeling that can be used for expansion to full field displacement as well as stress–strain prediction. This efficient approximation and modeling of structures is a result of recent developments in the computation of reduced order model response which allows for the accurate calculation of system's time response while retaining all the highly refined and complex characteristics of full finite element models. Work by Thibault [1–3] and Marinone [4–6] showed that system level response can be accurately and efficiently calculated for highly reduced system models. Moreover, Pingle [7–12] and Carr [13–16] demonstrated that the expansion of such systems can be used for the prediction of full field results as well as stress and strain from limited sets of data. Harvie and Avitabile [17–20] extended this work to include the application of expansion to nonlinear systems made out of linear components but subjected to nonlinear interactions. In that work, the expansion was greatly simplified by using the unconnected component modes to expand the response of the reduced system model as developed by Nonis [21, 22].

In this paper, multi-component structural systems are addressed in the context of retaining embedded structural information of ancillary subcomponents for the calculation of nonlinear reduced order model time response. For linear forced response, expansion was shown to return a precise approximation of the ancillary subcomponent even in cases where the reduction does not include active DOF at that subcomponent level [23]. A full space finite element model consisting of two systems, one of which contains a dynamically active ancillary subcomponent, will be reduced to a smaller set of degrees freedom and used for the prediction of the forced time response of the system as seen in Fig. 3.1. Gap-spring contact elements are introduced to generate nonlinear response between the two systems. The reduced order model (with embedded ancillary subcomponent information) will then be used to calculate the response at ADOF and then to expand back to the full space finite element model and to extract the predicted forced response of the ancillary subcomponent. This study will use SEREP [24] and ERMT (Equivalent Reduced Modeling Technique [1]) for reduction/expansion and characterization of the subsystem components from the available reduced system information.

The advantages of using reduced order models can be seen from a substantial reduction in computation time even when such systems involve nonlinear effects. The selection of degrees of freedom during the reduction process will explore whether it is necessary to include the connecting degrees of freedom of the ancillary component and the larger coupling structure or if these can be omitted as long as the preserved modes of the reduced system span the space of all modes of interest of the system. This is of particular importance in real life experimentation, as often times, measurements cannot be made exactly at the connecting degrees of freedom of multi-component structures or highly detailed finite element models are necessary to approximate the behavior of the system at those locations.

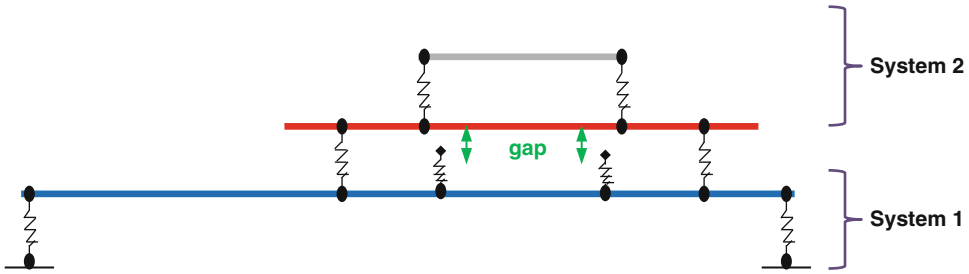

Fig. 3.1 Three beam structure consisting of two systems with active ancillary subcomponent in *grey*

3.2 Theory

The fundamentals of the study of forced response estimation and expansion/reduction of linear and nonlinear systems require a variety of theoretical topics briefly presented here. The summary starts with a description of linear multiple degree of freedom systems and continues with an overview of system modeling and mode contribution, structural dynamic modification, analytical model reduction and expansion, expansion of system modes from uncoupled component modes, forced time response computations and time correlation tools. Further information can be found in the respective references.

3.2.1 Equations of Motion for Multiple Degree of Freedom System

The general equation of motion for a multiple degree of freedom system written in matrix form is

$$[M_1]\{\ddot{x}\} + [C_1]\{\dot{x}\} + [K_1]\{x\} = \{F(t)\} \tag{3.1}$$

Assuming proportional damping, the eigensolution is obtained from

$$[\,[K_1] - \lambda\,[M_1]\,]\{x\} = \{0\} \tag{3.2}$$

The eigensolution yields the eigenvalues (natural frequencies) and eigenvectors (mode shapes) of the system. The eigenvectors are arranged in column fashion to form the modal matrix $[U_1]$. Often times, only a subset of modes is included in the modal matrix to save on computation time and due to the fact that only certain modes actually contribute to the response. Exclusion of modes results in truncation error which can be serious if key modes are excluded. Truncation error will be discussed in further detail in the structural dynamic modification section.

The physical system can be transformed to modal space using the modal matrix as

$$[U_1]^T[M_1][U_1]\{\ddot{p}_1\} + [U_1]^T[C_1][U_1]\{\dot{p}_1\} + [U_1]^T[K_1][U_1]\{p_1\} = [U_1]^T\{F(t)\} \tag{3.3}$$

Scaling to unit modal mass yields

$$\begin{bmatrix} \ddots & & \\ & I_1 & \\ & & \ddots \end{bmatrix}\{\ddot{p}_1\} + \begin{bmatrix} \ddots & & \\ & 2\xi\omega_n & \\ & & \ddots \end{bmatrix}\{\dot{p}_1\} + \begin{bmatrix} \ddots & & \\ & \Omega_1^2 & \\ & & \ddots \end{bmatrix}\{p_1\} = \left[U_1^n\right]^T\{F(t)\} \tag{3.4}$$

where $[I_1]$ is the diagonal identity matrix, $[{\Omega_1}^2]$ is the diagonal natural frequency matrix and $[2\xi\omega_n]$ is the diagonal damping matrix (assuming proportional damping). More detailed information on the equation development is contained in Ref. [25].

3.2.2 System Modeling and Mode Contribution

The approach used for the prediction of the nonlinear system response uses concepts from system modeling. In order to create multi-component models, various techniques are available for the coupling of several component models into a single

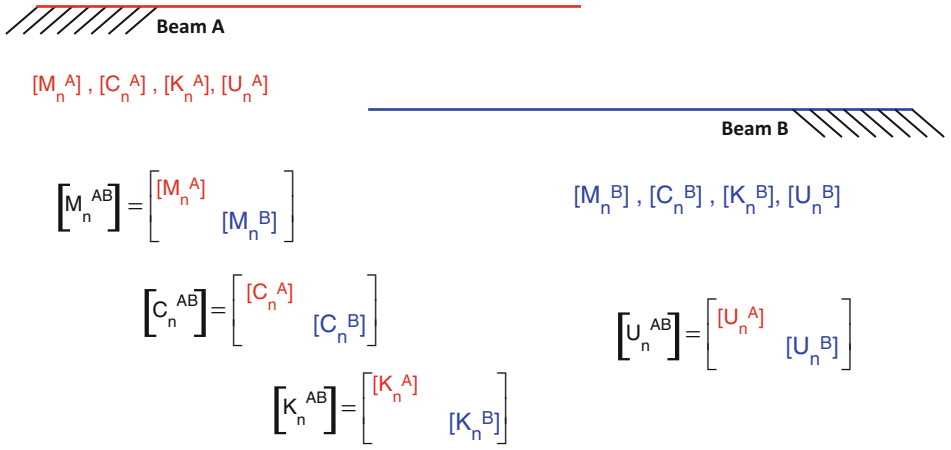

Fig. 3.2 Sample components arranged into common matrix space

system model. These system modeling techniques are used to define the various states that the system will undergo when the different nonlinear contact connections occur. The system modeling can be performed in physical space, modal space, or a combination of both physical and modal space. Consider two beams that are completely independent of one another, as illustrated in Fig. 3.2.

The two beams shown in Fig. 3.2 are completely uncoupled and will respond independent of one another when excited. A system model of the uncoupled components is generated by simply writing the variables in common matrix space, as shown in the diagram. To generate a coupled system model, specific coupling terms must be introduced at the desired locations. To include the spring(s) in the system modeling, either a modal or physical approach can be employed. The modal approach involves using Structural Dynamic Modification (SDM) and Component Mode Synthesis (CMS). The physical approach involves using a physical tie matrix to couple the beams. Both approaches involve the use of a mode contribution matrix to determine the appropriate number of component modes that contribute to the system modes. For the results presented here, physical system modeling techniques were used to generate databases for the various configurations.

3.2.2.1 Physical Space System Modeling

To form a physical system model, the mass and stiffness matrices of each component (A and B) are assembled in stacked form into the system mass and stiffness matrices. In physical space, these are coupled with a stiffness tie matrix; a mass tie can also be included if desired but not included in this work.

$$\left[\begin{bmatrix}[M^A] & \\ & [M^B]\end{bmatrix}\right]\{\ddot{x}\} + \left[\begin{bmatrix}[K^A] & \\ & [K^B]\end{bmatrix} + K_{TIE}\right]\{x\} = \{F\} \tag{3.5}$$

This can be cast in a modal space representation as

$$\left[\begin{bmatrix}[\overline{M}^A] & \\ & [\overline{M}^B]\end{bmatrix}\right]\begin{Bmatrix}\{\ddot{p}^A\} \\ \{\ddot{p}^B\}\end{Bmatrix} + \left[\begin{bmatrix}[\overline{K}^A] & \\ & [\overline{K}^B]\end{bmatrix}\right]\begin{Bmatrix}\{p^A\} \\ \{p^B\}\end{Bmatrix} + \left[[U]^T[\Delta K][U]\right]\begin{Bmatrix}\{p^A\} \\ \{p^B\}\end{Bmatrix} = \{0\} \tag{3.6}$$

where $[\overline{M}]$ and $[\overline{K}]$ are diagonal matrices and with the mode shapes of each component stacked as

$$[U] = \begin{bmatrix}[U^A] & \\ & [U^B]\end{bmatrix} \tag{3.7}$$

Equation 3.5 is a general equation of motion in physical space; Eq. 3.6 is the modal space equation used for the eigensolution.

3.2.2.2 Structural Dynamic Modification

Structural Dynamic Modification (SDM) is a technique that uses the original mode shapes and natural frequencies of a system to estimate the dynamic characteristics due to changes in the mass and/or stiffness of the system. First, the change of mass and stiffness are transformed to modal space as shown

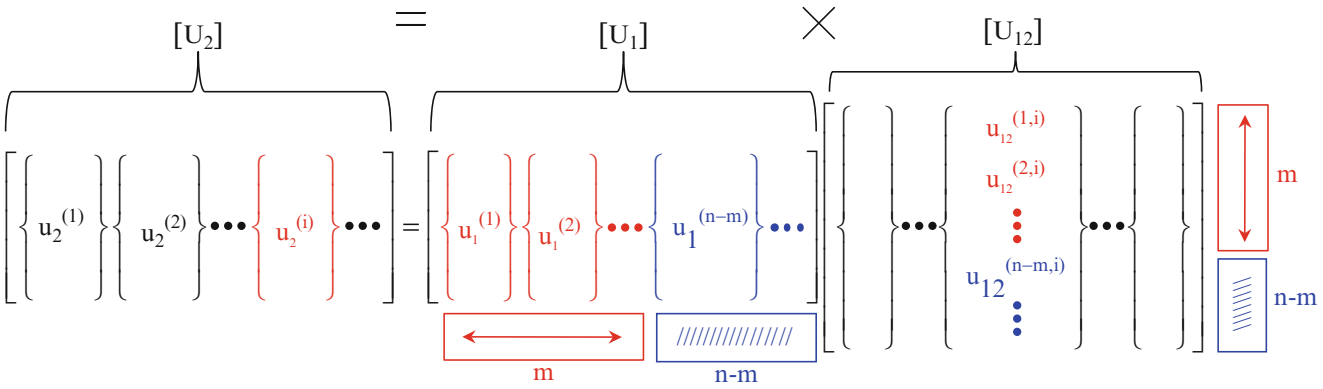

Fig. 3.3 Structural dynamic modification, mode contribution identified using U_{12} [2]

$$\left[\Delta\overline{M}_{12}\right] = [U_1]^T \left[\Delta M_{12}\right] [U_1] \tag{3.8}$$

$$\left[\Delta\overline{K}_{12}\right] = [U_1]^T \left[\Delta K_{12}\right] [U_1] \tag{3.9}$$

The modal space mass and stiffness changes are added to the original modal space equations as seem in Eq. 3.6 to obtain

$$\left[\begin{bmatrix} \ddots & & \\ & \overline{M}_1 & \\ & & \ddots \end{bmatrix} + \left[\Delta\overline{M}_{12}\right]\right] \{\ddot{p}_1\} + \left[\begin{bmatrix} \ddots & & \\ & \overline{K}_1 & \\ & & \ddots \end{bmatrix} + \left[\Delta\overline{K}_{12}\right]\right] \{p_1\} = [0] \tag{3.10}$$

The eigensolution of the modified modal space model is computed and the resulting eigenvalues are the new frequencies of the system. The resulting eigenvector matrix is the $[U_{12}]$ matrix, which is used to transform the original modes to the new modes as indicated by

$$[U_2] = [U_1]\ [U_{12}] \tag{3.11}$$

The new mode shapes are $[U_2]$. The new mode shapes are formed from linear combinations of the original mode shapes. The $[U_{12}]$ matrix shows how much each of the $[U_1]$ modes contributes to forming the new modes. Figure 3.3 shows the formation of the new mode shapes as seen on Eq. 3.11. Reference [25] has additional information on SDM.

The mode contribution matrix is used to determine which original mode shapes are necessary for the accurate reconstruction of each of the desired final mode shapes. If a dynamic response involves multiple system states, then the $[U_{12}]$ matrix must be computed for each configuration to determine the number of original system modes to appropriately span the space of the solution and avoid truncation.

3.2.3 General Reduction/Expansion Methodology and Model Updating

Model reduction is a tool used to reduce the number of degrees of freedom (DOF) in order to minimize the required computation time of an analytical model, while attempting to preserve the full DOF dynamic characteristics. The relationship between the full space and reduced space model can be written as

$$\{X_n\} = \begin{Bmatrix} X_a \\ X_d \end{Bmatrix} = [T]\{X_a\} \tag{3.12}$$

where subscript 'n' signifies the full set of DOF (NDOF), 'a' signifies the reduced set of DOF (ADOF) and 'd' is the deleted DOF (those DOF not used during the reduced computation process). The transformation matrix [T] relates the full set of NDOF to the reduced set of ADOF. The transformation matrix is used to reduce the mass and stiffness matrices as

$$[M_a] = [T]^T [M_n] [T] \text{ and } [K_a] = [T]^T [K_n] [T] \tag{3.13}$$

The eigensolution of these 'a' set mass and stiffness matrices are the modes of the reduced model. These modes can be expanded back to full space using the transformation matrix

$$[U_n] = [T\,] [U_a] \tag{3.14}$$

If an optimal 'a' set is not selected when using methods such as Guyan Condensation [26] or Improved Reduced System Technique [27], the reduced model may not perfectly preserve the dynamics of the full space model. If System Equivalent Reduction Expansion Process (SEREP) [24] is used, the dynamics of selected modes will be perfectly preserved regardless of the 'a' set selected as long as the matrix is formed from a linearly independent set of vectors. Some additional information regarding the DOF selection in regards to expansion is studied in a companion paper [28].

3.2.3.1 Expansion of System Modes from Uncoupled Component Modes

Expansion is generally used for providing full N-space mode shape information extracted from limited a-space information. The expansion to full space in this paper is based on recent work by Nonis [19, 20] showing that full N-space mode shape information for an assembled system model can be obtained using the expansion matrices from the uncoupled, unconnected, original component modes of each component. Figure 3.4 shows the entire expansion process schematically to further describe the overall procedure. Ref. [19] further details the expansion process and considerations for modes included.

While the systems studied here undergo several configurations, the expansion can be performed with a single transformation matrix obtained from the original unconnected unmodified systems. As long as the modes retained during the reduction process span the space of the full space solution of the system, the transformation matrix will produce accurate expanded predictions of the multi-configuration response. Using a single transformation matrix of the unconnected individual components/systems is much more efficient since the full space modes of the connected system are not computed.

3.2.3.2 System Equivalent Reduction Expansion Process (SEREP)

The SEREP modal transformation relies on the partitioning of the modal equations representing the system using selected DOFs and modes to obtain a reduced model that perfectly preserves the eigenvalues and eigenvectors of interest [24]. The SEREP technique utilizes the mode shapes from a full finite element solution to map to the limited set of active DOF. SEREP is not performed to achieve efficiency in the solution but rather is intended to perform an accurate mapping matrix for the transformation. The SEREP transformation matrix is formed using a subset of modes at full space and reduced space as

$$[T_U] = [U_n] [U_a]^g \tag{3.15}$$

where $[U_a]^g$ is the generalized inverse and $[T_U]$ is the SEREP transformation matrix. When the SEREP transformation matrix is used for model reduction/expansion as outlined in the previous section, the reduced model perfectly preserves the full space dynamics of the modes in $[U_n]$ [24].

3.2.4 System Forced Response Analysis

The computation of the time response developed in this paper is based on the Equivalent Reduced Model Technique (ERMT), a technique developed by Avitabile and Thibault [1–4]. This technique uses an exact reduced model representation for the calculation of the system response. Newmark integration technique [29] is used to perform the direct integration of the equations of motion for the ERMT solution process. From the known initial conditions for displacement and velocity, the initial acceleration vector is computed using the equation of motion and the applied forces as

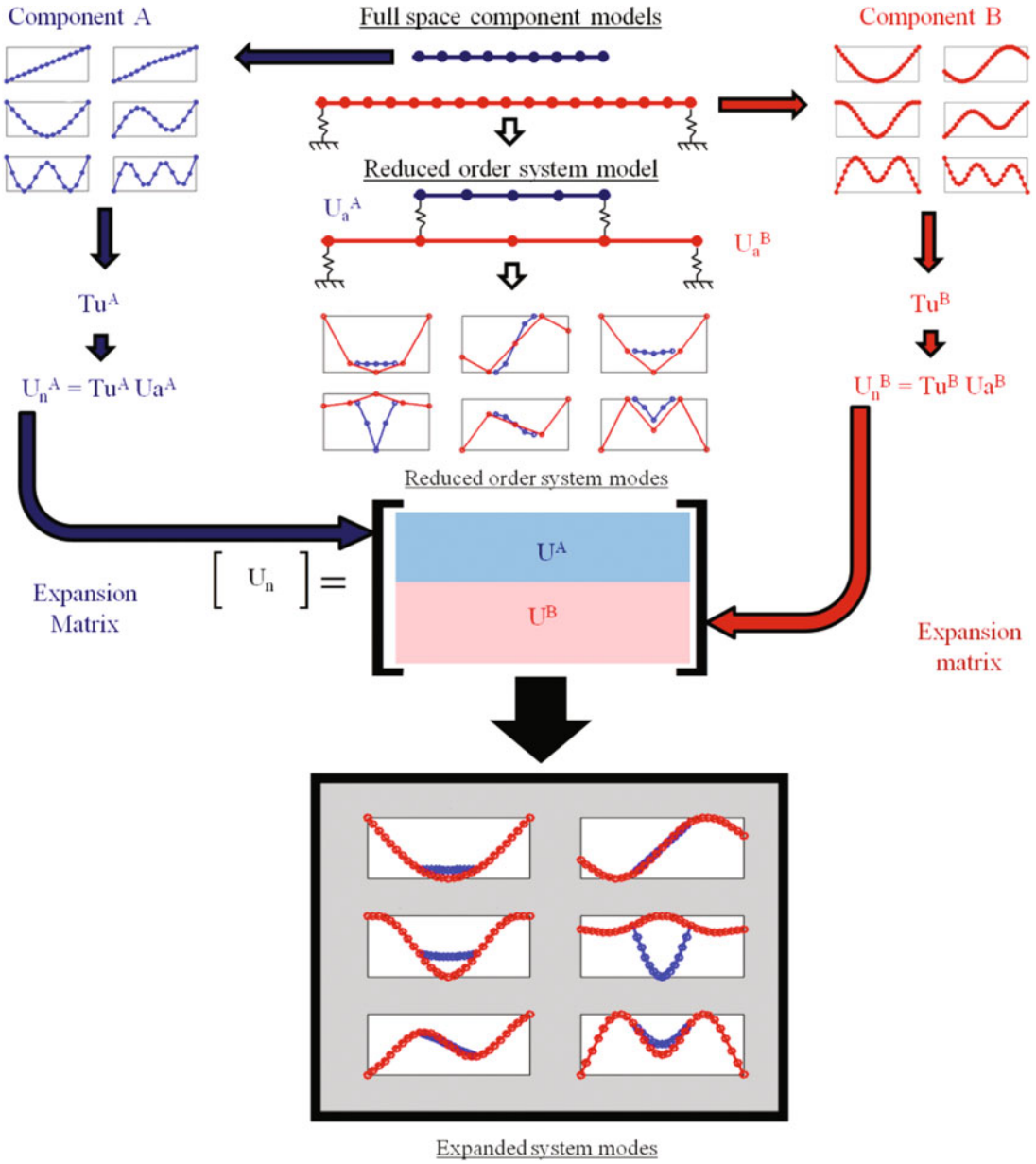

Fig. 3.4 Overall expansion process schematic using the transformation matrices from unconnected system components

$$\ddot{\vec{x}}_0 = [M]^{-1}\left(\vec{F}_0 - [C]\ \dot{\vec{x}}_0 - [K]\ \vec{x}_0\right) \tag{3.16}$$

Choosing an appropriate Δt, α, and β, the displacement vector is

$$\begin{aligned}\vec{x}_{i+1} = &\left[\tfrac{1}{\alpha(\Delta t)^2}[M] + \tfrac{\beta}{\alpha(\Delta t)}[C] + [K]\right]^{-1}\\ &\left\{\vec{F}_{i+1} + [M]\ \left(\left(\tfrac{1}{\alpha(\Delta t)^2}\right)\vec{x}_i + \left(\tfrac{1}{\alpha(\Delta t)}\right)\dot{\vec{x}}_i + \left(\tfrac{1}{2\alpha} - 1\right)\ddot{\vec{x}}_i\right)\right.\\ &\left. + [C]\ \left(\left(\tfrac{\beta}{\alpha(\Delta t)}\right)\vec{x}_i + \left(\tfrac{\beta}{\alpha} - 1\right)\dot{\vec{x}}_i + \left(\tfrac{\beta}{\alpha} - 2\right)\tfrac{\Delta t}{2}\ddot{\vec{x}}_i\right)\right\}\end{aligned} \tag{3.17}$$

The values chosen for α and β were ¼ and ½, respectively. This assumes constant acceleration and the integration process is unconditionally stable, where a reasonable solution will always be reached regardless of the time step used. However, the

time step should be chosen such that the highest frequency involved in the system response can be characterized properly to avoid numerical damping in the solution.

Following the displacement vector calculation, the acceleration and velocity vectors are computed for the next time step using

$$\dot{\vec{x}}_{i+1} = \dot{\vec{x}}_i + (1-\beta)\,\Delta t\,\ddot{\vec{x}}_i + \beta \Delta t\,\ddot{\vec{x}}_{i+1} \tag{3.18}$$

$$\ddot{\vec{x}}_{i+1} = \frac{1}{\alpha(\Delta t)^2}\left(\vec{x}_{i+1} - \vec{x}_i\right) - \frac{1}{\alpha \Delta t}\,\dot{\vec{x}}_i - \left(\frac{1}{2\alpha} - 1\right)\ddot{\vec{x}}_i \tag{3.19}$$

This process is repeated at each time step for the duration of the time response solution desired.

3.2.5 *Expansion of Reduced Order Real Time Response*

Chipman [30–33] and others [1–18] showed that a transformation matrix can be used to expand not only mode shapes, but dynamic time response data. Therefore the same principles presented above can be extended to the expansion of coupled response using uncoupled component information. The response of the coupled system at reduced space can be expanded to full space using the transformation matrices of the individual, unconnected beams systems because the dynamic characteristics of the system are directly related to the dynamic characteristics of the uncoupled components. If the $[U_{12}]$ matrix is evaluated to include enough modal information in the reduced model to accurately represent the system with the coupling elements present, then the time response of the coupled system is accurately expanded to full space using information from the uncoupled components.

For this work, nonlinear systems are analyzed where several possible configurations can exist during response. If all possible configurations are made up of linear combinations of the component mode shapes, then the expansion of nonlinear response of a reduced model can be expanded using the original transformation matrix regardless of the configurations encountered. Figure 3.5 shows the process for determining full space dynamic response of a nonlinear system using the original transformation matrices. The nonlinear contacts in green (Fig. 3.5) indicate when the spring comes in contact with the structure and thus changes from one configuration to another. Although several configurations exist within the time block shown, all modified states can be generated based on the mode shapes of the original system. Therefore only the transformation matrices of the original, uncoupled components are necessary to expand the nonlinear dynamic response of the system regardless of the configurations encountered.

3.2.6 *Time Response Correlation Tools*

In order to quantitatively compare two different time solutions, two correlation tools were employed: The Modal Assurance Criterion (MAC) and the Time Response Assurance Criterion (TRAC).

3.2.6.1 Modal Assurance Criterion (MAC)

The Modal Assurance Criterion (MAC) [34] is widely used as a vector correlation tool. In this work, the MAC was used to correlate all DOF at a single instance in time. The MAC is written as

$$MAC_{ij} = \frac{\left[\{X1_i\}^T \{X2_j\}\right]^2}{\left[\{X1_i\}^T \{X1_i\}\right]\left[\{X2_j\}^T \{X2_j\}\right]} \tag{3.20}$$

where X1 and X2 are displacement vectors. MAC values close to 1.0 indicate strong similarity between vectors, where values close to 0.0 indicate minimal or no similarity.

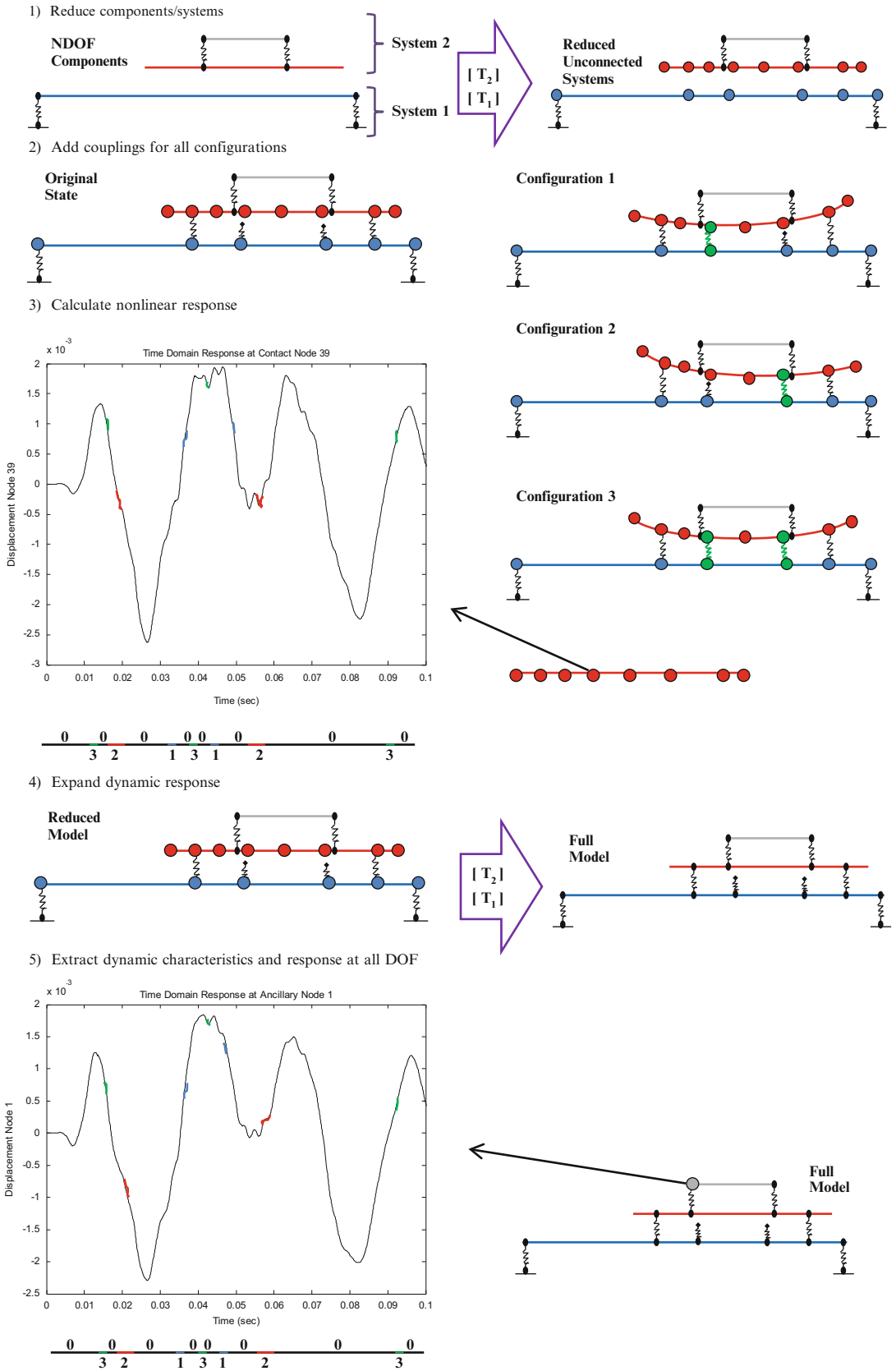

Fig. 3.5 Expansion of nonlinear response using system component mode shapes

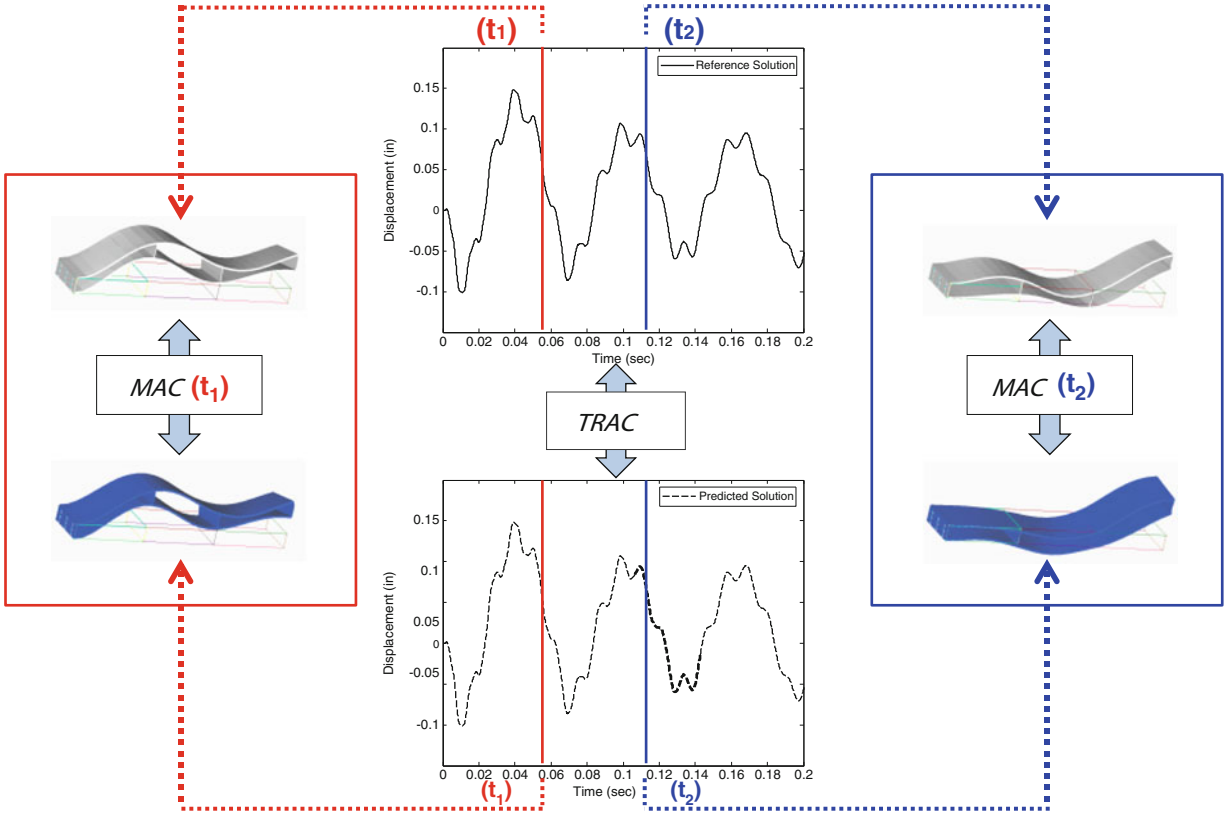

Fig. 3.6 Physical interpretation of MAC and TRAC

3.2.6.2 Time Response Assurance Criterion (TRAC)

The Time Response Assurance Criterion (TRAC) [35] quantifies the similarity between a single DOF across all instances in time. The TRAC is written as

$$\mathrm{TRAC}_{ji} = \frac{\left[\{X1_j(t)\}^T \{X2_i(t)\}\right]^2}{\left[\{X1_j(t)\}^T \{X1_j(t)\}\right]\left[\{X2_i(t)\}^T \{X2_i(t)\}\right]} \tag{3.21}$$

where X1 and X2 are time response vectors for a particular DOF. TRAC values close to 1.0 indicate strong similarity between vectors, where values close to 0.0 indicate minimal or no similarity.

In this work, the MAC is calculated between the shapes of the full space reference solution and estimated solution obtained from the reduced order model at each time step. Similarly the TRAC is used to compare the time response from the reduced order model to the time response from the full space finite element solution at each degree of freedom. A diagram detailing the two comparison techniques is shown in Fig. 3.6.

3.3 Model Description

Analytical models of a multi-component beam system were created to investigate the prediction of the dynamic response of the system including subcomponents and ancillary attachments. The models consisted of 3 beams, as illustrated in Fig. 3.1, attached asymmetrically by linear springs and such that all components are dynamically active. SEREP was used for all reduced models. Planar element beam models of the cantilevered beam were generated using MAT_SAP [36], which is a FEM program developed for MATLAB [37], and forced response calculations were performed in MATLAB using Newmark

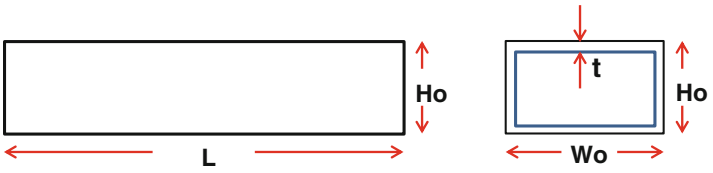

Fig. 3.7 Dimensions of top (*red*) and support/base(*blue*) beams of the analytical beam system

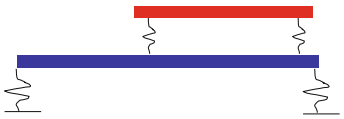

Property of Beam	Beam A	Beam B
Wo - Beam width (in)	2	3
Ho - Beam height (in)	1	4
t - Wall thickness (in)	3/8	1/8
L - Length(in)	50	140
E – Young's Modulus	10e6 psi	
ρ – Weight density	0.1 lb/in^3	
# of elements	20	70

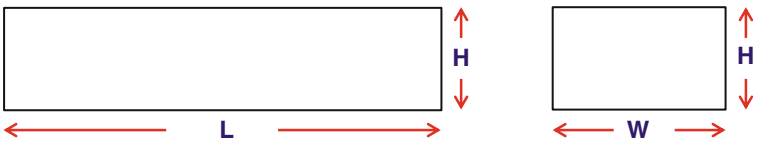

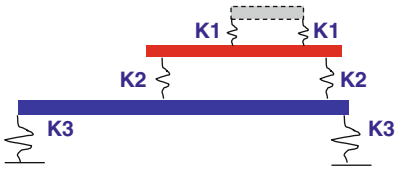

K1 & K2 = 1e6 lb/in
K3 = 1e3 lb/in

Fig. 3.8 Dimensions and characteristics of ancillary subcomponent (*grey*) of 3 beam system

Ancillary Beam Dimensions and Physical Properties	
L – Length	15 in
H – Height	0.25 in
W – Width	0.5 in
E – Young's Modulus	10e6 psi
ρ – Weight density	0.1 lb/in^3
# of Elements	10

integration scripts. The beam models were set to have dimensions and characteristics as described in Figs. 3.7 and 3.8. For all models 1 % of critical damping was used in the time response computation.

The system was subjected to a double sided force pulse at the tip of the blue beam (lowest beam) and this input force was designed as to only excite the modes in a frequency band of approximately 250 Hz as shown in Fig. 3.9. The table of frequencies for each separatecomponent and full assembled system (with and without the ancillary) can be seen in Table 3.1.

With all 100 elements of the system (i.e. 206 DOF) the full N-space reference solution to the system was calculated and served as a point of comparison for all subsequent reduced order model calculations. The nonlinear contacts were setup in two configurations, one where the contacts occurs between the blue and red beam (Case A) and one where the contact takes place at the subcomponent level (Case B) as seen in Fig. 3.10. The soft contacts are springs with a stiffness of 100 lb/in, while the hard contacts have a stiffness of 10,000 lb/in.

As studied in [23], for the linear forced response of this multi-component system the connecting DOF as well as DOF at the ancillary subcomponent are not needed in order to accurately predict the system level response. Similar conclusion will be drawn in this work, extending the prediction of the subcomponent response for nonlinear cases. However, in the nonlinear cases studied here, the location of the nonlinearity can have a significant effect on the accuracy of the prediction and on the number of modes (and DOF) required in the reduction/expansion process.

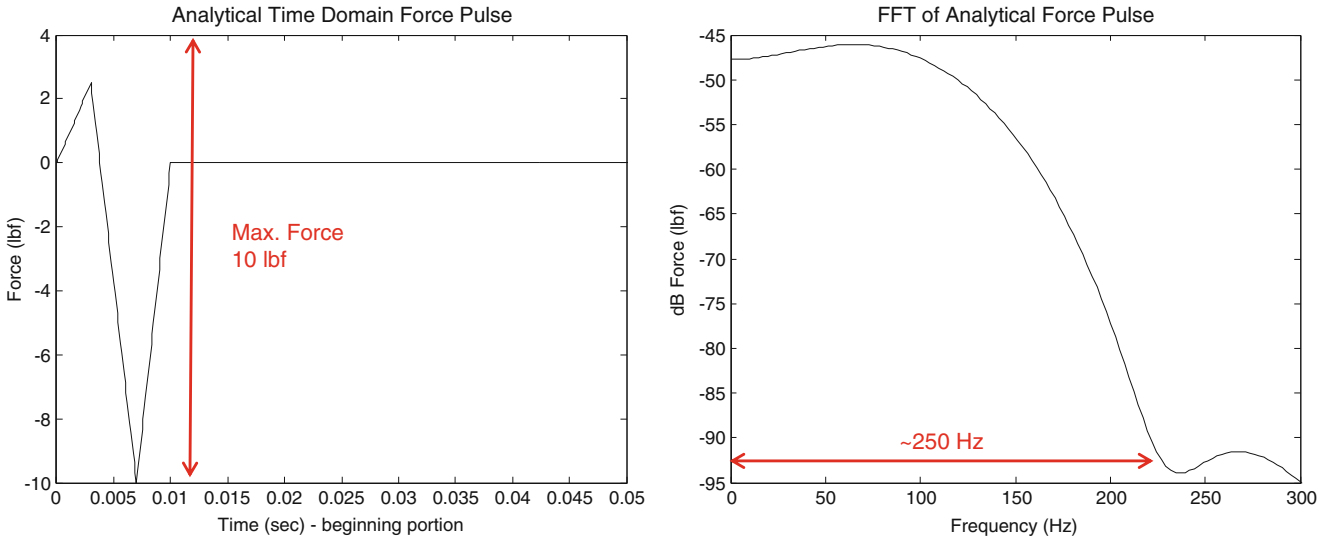

Fig. 3.9 Time (*left*) and frequency (*right*) domain plots of input analytical force pulse

Table 3.1 Frequencies of the first 15 modes of the 3 beam system (with and without ancillary) and its components

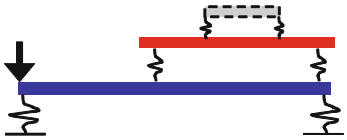

Mode	Frequency (Hz)				
	Beam A	**Beam B**	**Ancillary**	**System w/o A.C.**	**System**
1	0.0015	18.9	0.010	16.8	16.8
2	0.0024	45.9	0.014	37.6	37.5
3	87.6	80.9	224.5	68.2	68.1
4	241.4	161.4	619.0	86.9	84.6
5	473.2	299.7	1,214.3	129.1	102.1
6	782.3	489.4	2,010.4	210.5	129.1
7	1,168.8	728.2	3,011.1	282.8	210.0
8	1,633.1	1,015.5	4,223.0	343.1	282.0
9	2,175.4	1,351.0	5,653.7	477.1	343.0
10	2,796.3	1,734.7	7,302.3	645.5	396.2
11	3,496.7	2,166.4	9,071.4	716.4	477.3
12	4,277.7	2,646.2	12,046.9	959.5	645.3
13	5,140.7	3,174.1	14,493.9	1,118.7	716.3
14	6,087.4	3,750.0	17,502.7	1,311.7	88–9.0
15	7,120.0	4,373.9	21,038.3	1,617.3	960.6

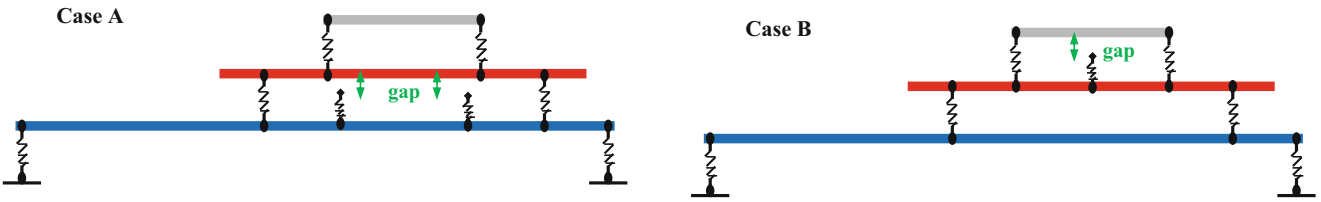

Fig. 3.10 Nonlinear gap-spring contact cases analyzed

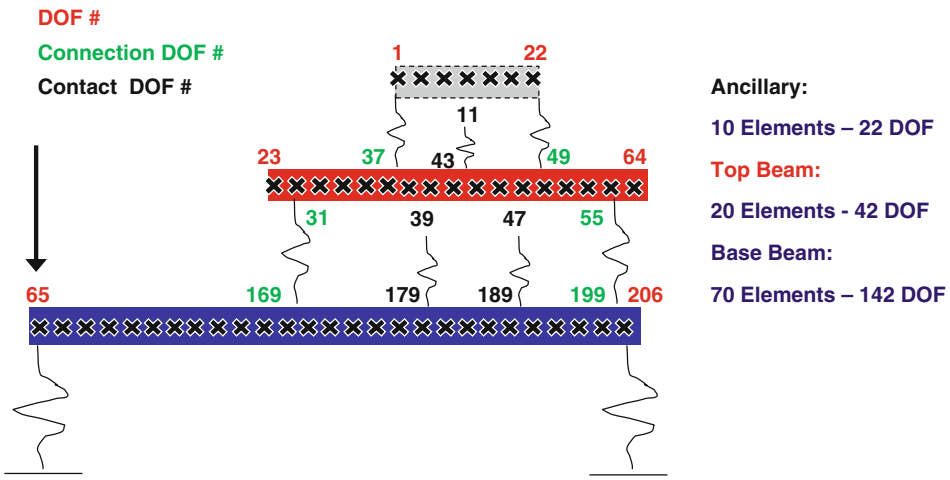

Fig. 3.11 Numbering scheme of three beam system at NDOF (206) with connection and contact locations

3.4 Cases Studied

Two nonlinear configurations of the three beam system were analyzed as shown in Fig. 3.10. The forced response of the full space reference models with 206 DOF were calculated first. Structural Dynamic Modification was used to calculate the $[U_{12}]$ matrix for each configuration of Case A and Case B. For Case A, four different configurations are possible as shown in Fig. 3.5. Similarly, Case B has two possible different configurations.

Using the calculated $[U_{12}]$ for all configurations, the necessary number of component modes were determined in order to properly characterize the system; using the force described above, the system modes must be able to characterize the response over a 250 Hz frequency span. While this is the initial frequency range of interest for any structural dynamic study, there also needs to be consideration for the nonlinear contacts which occur that may require a frequency range beyond that initially determined from the applied forcing function.

SEREP reduction was used to reduce the active DOF of the system to an 'a' set not including DOFs on the ancillary beam (except when noted). The forced responses of the reduced ADOF systems were computed. The dynamic characteristics of the ancillary subcomponent were then extracted using the system information available from the reduction process. The test cases presented here are intended to show the results when a proper set of modes are selected such that no information is lost in the reduction process as well as inaccurate reduced models where the modes do not span the full space response of the system. The arrangement of DOF and connecting DOF is illustrated in Fig. 3.11.

The cases presented here are summarized as:

Case A: Two Nonlinear Contacts Between System 1 and System 2

Case A-1: Soft Contact Reference Solution

206 DOF Total; System 1/Beam B 142 DOF; System 2 – Beam A 42 DOF and Ancillary 22 DOF.
Nonlinear Contacts of 100 lb/in at Beam A DOF 39 and 47 of System 2.

Case A-1.1: Soft Contact Reduced Model Solution with 12 Modes

12 DOF Total; Beam B – ADOF 65, 169, 179, 189, and 199;
Beam A – ADOF 23, 31, 39, 43, 47, 55 and 63.
Nonlinear Contacts of 100 lb/in at Beam A ADOF 39 and 47 of System 2.

Case A-1.2: Soft Contact Reduced Model Solution with 16 Modes

16 DOF Total; Beam B – ADOF 65, 99, 135, 169, 179, 189, 199 and 205;
Beam A – ADOF 23, 31, 35, 39, 43, 47, 55 and 63.
Nonlinear Contacts of 100 lb/in at Beam A ADOF 39 and 47 of System 2.

Case A-2: Hard Contact Reference Solution

206 DOF Total; System 1/Beam B 142 DOF; System 2 – Beam A 42 DOF and Ancillary 22 DOF.
Nonlinear Contacts of 10,000 lb/in at Beam A DOF 39 and 47 of System 2.

Case A-2.1: Hard Contact Reduced Model Solution with 21 Modes

21 DOF Total; Beam B – ADOF 65, 79, 89, 99, 109, 119, 149, 159, 169, 179, 189, 199 and 205;
Beam A – ADOF 31, 33, 39, 43, 47, 55, 57 and 61.
Nonlinear Contacts of 10,000 lb/in at Beam A ADOF 39 and 47 of System 2.

Case B: One Nonlinear Contact at System 2
Case B-1: Soft Contact Reference Solution

206 DOF Total; System 1/Beam B 142 DOF; System 2 – Beam A 42 DOF and Ancillary 22 DOF.
Nonlinear Contact of 100 lb/in at Ancillary DOF 11 of System 2.

Case B-1.1: Soft Contact Reduced Model Solution with 22 Modes with ADOF at Ancillary

22 DOF Total; Beam B – Modes 1–9 + 12, ADOF 65, 97, 117, 137, 157, 169, 177, 185, 199 and 205; Beam A – Modes 1–10 + 13 + 16, ADOF 11, 23, 29, 31, 33, 39, 43, 47, 51, 53, 55 and 63.
Nonlinear Contact 100 lb/in at Ancillary DOF 11 of System 2.

Case B-1.2: Soft Contact Reduced Model Solution with 18 Modes with No ADOF at Ancillary

18 DOF Total; Beam B – Modes 1–9 ADOF 65, 75, 97, 105, 127, 155, 169, 185, and 199;
Beam A – Modes 1–9 ADOF 25, 31, 35, 39, 43, 47, 53, 55 and 61.
Nonlinear Contact of 100 lb/in at Ancillary DOF 11 of System 2.

3.4.1 Case A: Two Nonlinear Contacts Between System 1 and System 2

3.4.1.1 Case A-1: Soft Contact Reference Solution

The NDOF unreduced subcomponents were tied together to form two systems, the support (System 1) and the top assembly (System 2). The frequencies and mode shapes of both untied and tied subcomponents were calculated for reference. The assembled 3 beam system consisting of the tied System 1 and System 2 was then tied together at full N-space and the nonlinear forced response calculated using the analytical input force of Fig. 3.9. The forced response of this NDOF (206 DOF) served as the reference solution for the reduced cases with two soft spring contacts (100 lb/in).

3.4.1.2 Component Mode Contribution – U_{12}

Calculation of the $[U_{12}]$ matrix for the system response is highly important to understand and mitigate the effects of truncation error in the reduction process. The modes from Systems 1 and System 2 required to preserve the first 5 modes of the assembled full 3 beam system were chosen using the resulting $[U_{12}]$ from all configurations (4 for Case A and 2 for Case B). Further considerations were made by taking the FFT of the response at the location of the input force and nonlinear contacts to verify if any additional modes were needed to characterize the system. As seen on the $[U_{12}]$ contribution matrix of Fig. 3.12, a total of 12 modes of the system components are required to preserve 5 modes of the assembled 3 beam system. Furthermore, mode 6 of System 2 has almost no contribution to the first 5 modes of the assembled system and could be excluded. System 1 (the blue support beam) contributes 5 modes to the reduced model while System 2 (the top red beam and its attached ancillary subcomponent) provides 7 modes. The larger contribution from system 2 is already an indication of the influence of the dynamics of the ancillary subcomponent. While some configurations required less modes than others, the maximum amount of modes in all configurations must be preserved. Moreover, Fig. 3.13 shows the FFT of the displacement

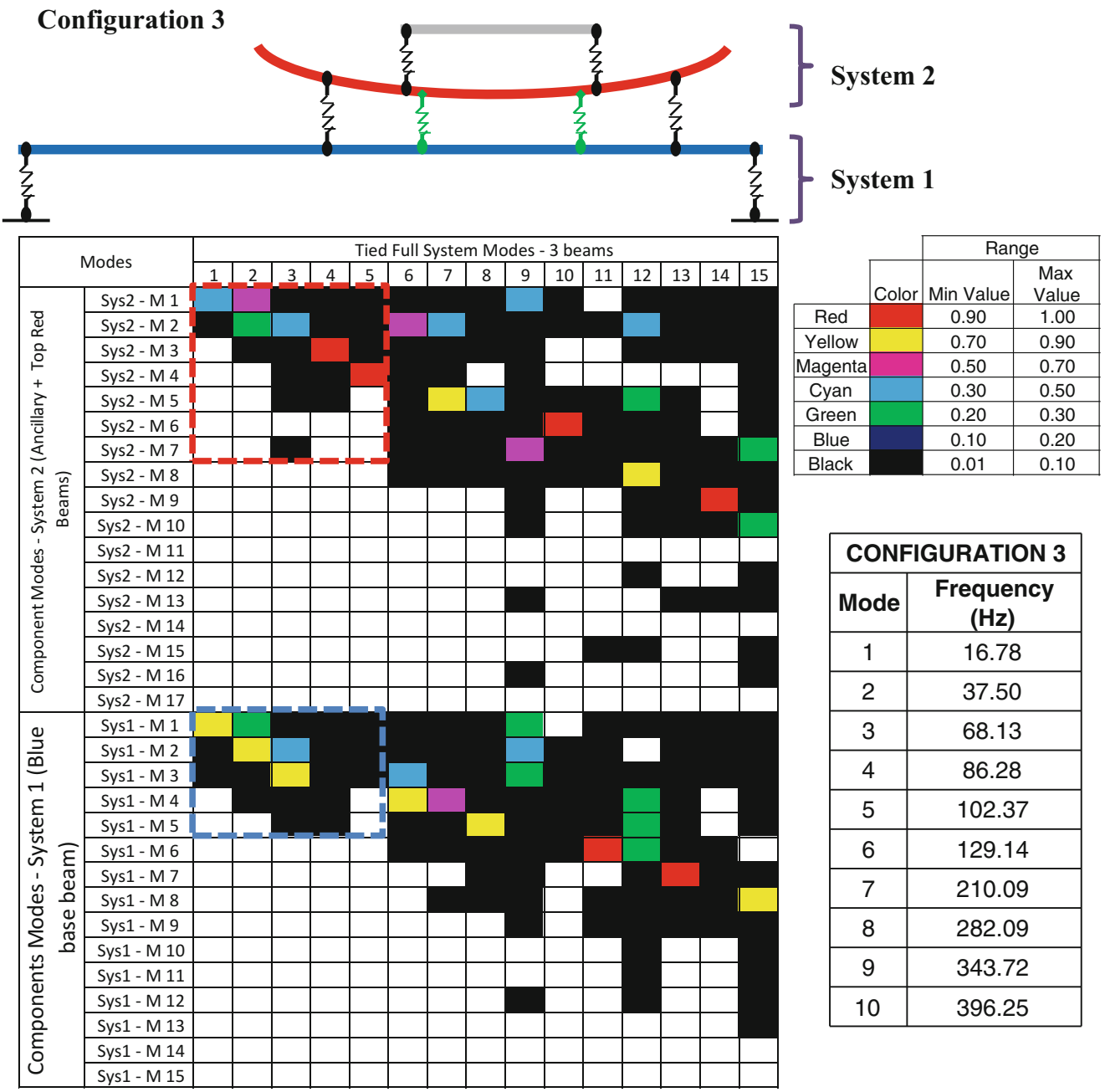

	Color	Range	
		Min Value	Max Value
Red		0.90	1.00
Yellow		0.70	0.90
Magenta		0.50	0.70
Cyan		0.30	0.50
Green		0.20	0.30
Blue		0.10	0.20
Black		0.01	0.10

CONFIGURATION 3	
Mode	**Frequency (Hz)**
1	16.78
2	37.50
3	68.13
4	86.28
5	102.37
6	129.14
7	210.09
8	282.09
9	343.72
10	396.25

Fig. 3.12 $[U_{12}]$ matrices for configurations 3 showing the maximum number of modes needed from the components of the assembled 3 beam system

at point 39 and 47 (contact location 1 and 2) for Case A-1 indicating the need of additional modes in the reduced models due to the activation of higher order modes.

The first 5 modes of the system are in a 100 Hz band as observed in Fig. 3.12. However, the input force pulse has an excitation range of approximately 250 Hz, while the contact locations show additional modes being active in the region of 100–300 Hz as seen in Fig. 3.13. As discussed above, the $[U_{12}]$ matrix indicates the need for 12 modes but as will be shown in the next case, additional modes are required for more accurate results.

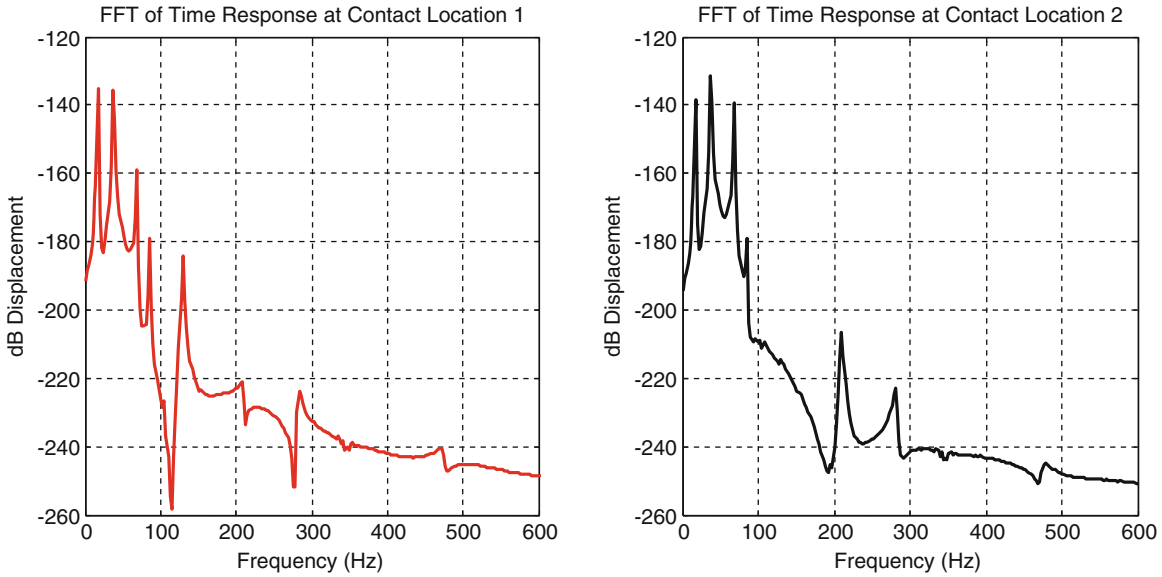

Fig. 3.13 FFT of reference time response at nonlinear soft contact locations

3.4.1.3 Overview of Reduction Process

The unconnected full space subcomponents (the 3 beams at NDOF) were first assembled into two components/assemblies, System 1 and System 2. The two systems are then connected and reduced to ADOF using SEREP reduction. The forced response is efficiently computed at ADOF and the transformation matrix of the unconnected components (obtained in the reduction process) is used to expand back to full space. The reduced models were created with emphasis in avoiding placement of active DOF at the ancillary subcomponent. The dynamics of this appendage must be predicted from the embedded information available in the reduction process. Moreover, note that only a single transformation matrix is needed for expansion even though the system goes through different configurations. This is possible because the mode shape projection vectors in the transformation matrix form a linearly independent set of vectors that span the space of the full space solution of the system. The process for the reduced model response calculation is shown in Fig. 3.14.

3.4.1.4 Case A-1.1: Soft Contact Reduced Model Solution with 12 Modes

A SEREP reduced model using 12 modes was created to illustrate the necessity for additional modes due to the interaction of the two contact springs in the response of the system. Using 12 modes for the system (5 from System 1 and 7 from System 2), the frequency range that is expected to have accurate time response prediction will likely only span about 100 Hz and is not really sufficient to obtain an accurate response. This case is included to clearly show that an appropriate set of modes must be selected otherwise poor results may be obtained; but this case does provide some results which are somewhat acceptable but can be greatly improved with the selection of more component modes which in turn provide better overall system modes. The ADOF selected were 23, 31, 39, 43, 47, 55 and 63 from Beam A and 65, 169, 179, 189, and 199 from Beam B. The nonlinear contacts occurred at ADOF 39 and 47 of System 2. Figure 3.15 shows the result of the expansion of this reduced model when compared to the full reference model of Case A-1.

While there is a good level correlation of the predicted response, the effect of the truncation of higher order modes is evident when taking a closer look at the response and FFT of the response at various points in the system. For instance, Fig. 3.16 shows the response at the contact 1 location. Using the information from the FFT and the $[U_{12}]$ matrix, a more accurate model can be obtained as will be shown in the next model.

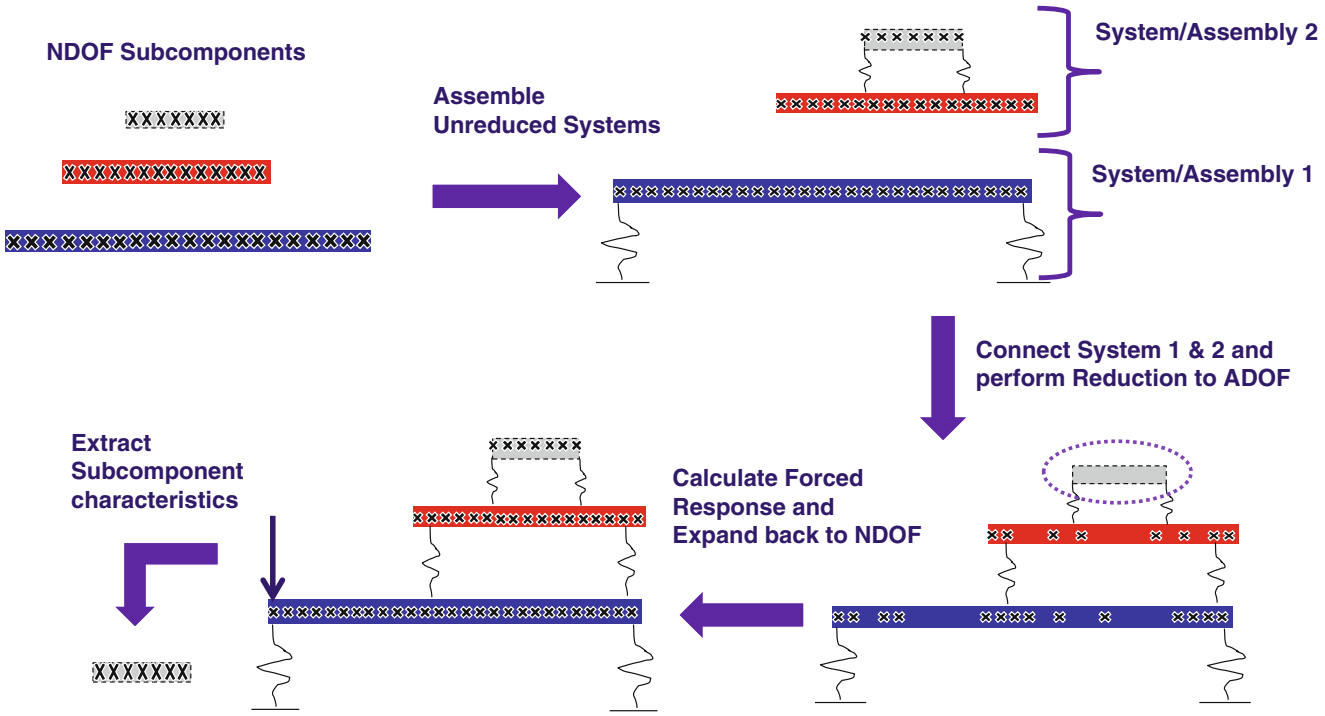

Fig. 3.14 Sequence for the development of reduced system response models

3.4.1.5 Case A-1.2: Soft Contact Reduced Model Solution with 16 Modes

A SEREP reduced model using 16 modes (8 from System 1 and 8 from System 2) was created in similar manner to that of the previous model (Case A-1.1). The ADOF selected were 23, 31, 35, 39, 43, 47, 55 and 63 from Beam A and 65, 99, 135, 169, 179, 189, 199 and 205 from Beam B. The nonlinear contacts occurred at ADOF 39 and 47 of System 2. Figure 3.17 shows the relevant portion of the $[U_{12}]$ matrix and Fig. 3.18 the comparison of the predicted response of the new model and the reference model.

Using 16 modes allows for the accurate prediction of up to 8 modes (which spans approximately 300 Hz) of the 3 beam assembled system. Comparing Figs. 3.15 and 3.18 show significant gain in accuracy across all DOF due to the addition of 4 modes to the reduced model. Figure 3.19 shows the comparison of the FFT of the displacement at the spring contact location 1 (in the same manner of that of Fig. 3.16).

The FFT of the displacement at contact location 1 in Fig. 3.19 shows that the effect of the mode truncation of the higher order modes has been highly reduced and the response is a more accurate approximation of the full NDOF solution. Note that no ADOF has been placed at the ancillary subcomponent or at the DOFs that connect the ancillary to Beam A but nevertheless the embedded information in the reduction process has successfully allowed the prediction of the time response at all NDOF.

The effect of higher order modes can be exacerbated if the type of contact is hard impact, thus producing a narrow time pulse that translates into a high order pulse in the frequency domain. The next case will explore a hard contact spring acting at two locations of the structure. A comparison of the two types of contacts, soft and hard, can be seen in Fig. 3.20.

3.4.1.6 Case A-2: Hard Contact Reference Solution

Nonlinear contacts of 10,000 lb/in were implemented instead of the soft contacts of 100 lb/in previously used. The response at NDOF was calculated for use as a reference in the next reduced model cases. New $[U_{12}]$ matrices were calculated for the 4 configurations of Case A using the hard contact. Taking the FFT of the displacement at the contact locations showed that the response is affected by a much larger range of modes as seen in Fig. 3.21.

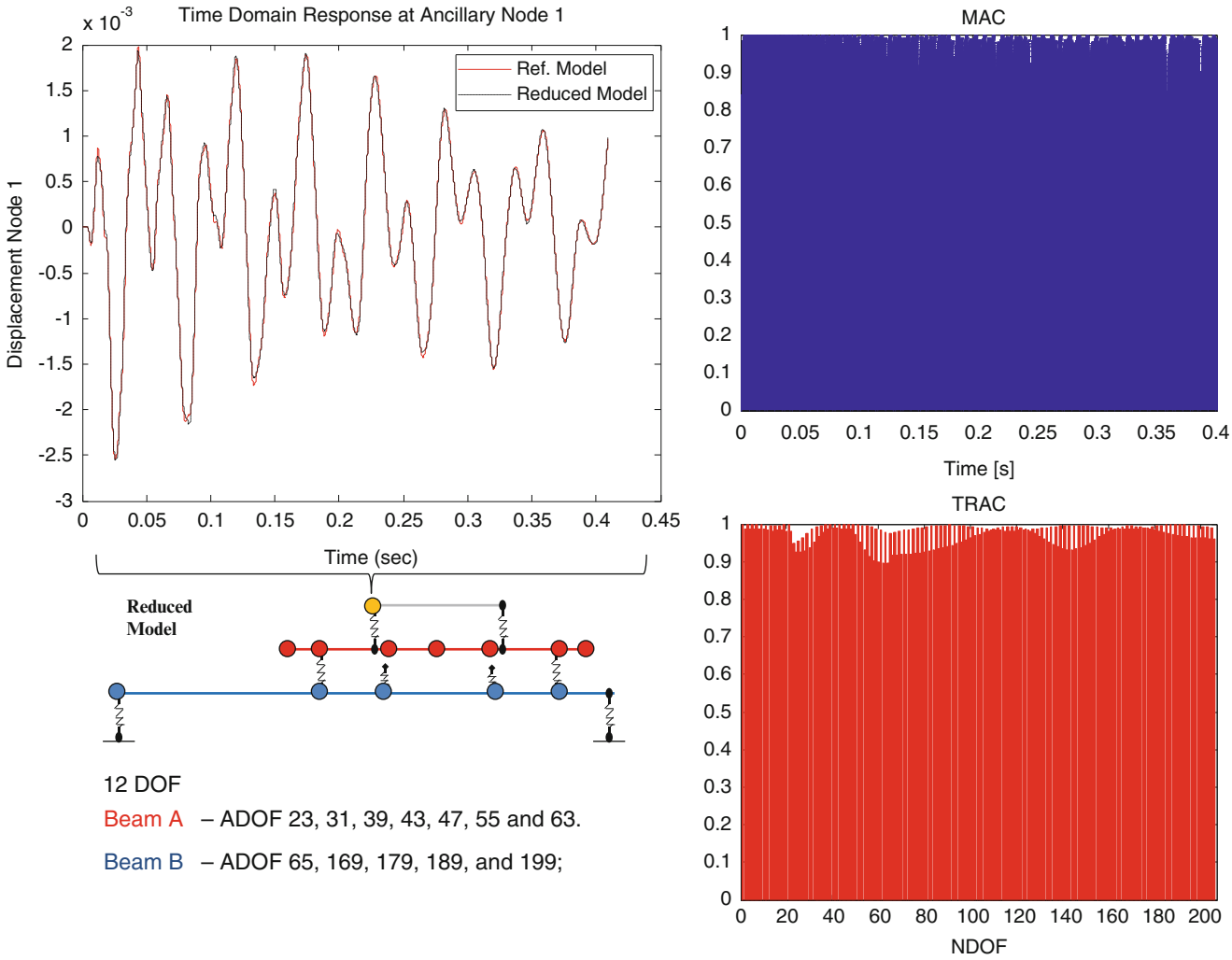

Fig. 3.15 Predicted response at ancillary from 12 DOF reduced model. MAC (*top right*) and TRAC (*bottom right*)

Figure 3.21 shows that the response of the 3 beam system with hard contacts involves high frequency modes well above 500 Hz which means up to 12 modes (or more) may be needed to accurately predict the response of the system. Figure 3.21 also list the frequencies of the hard contact case for the 4 possible configurations.

3.4.1.7 Case A-2.1: Hard Contact Reduced Model Solution with 21 Modes

Because the hard contact excites frequencies in the range of 700 Hz, the 14 or 16 mode models previously used cannot give the best approximation of the response of the system. The selection of modes preserved in the reduction must form a linearly independent set of vectors spanning the space of the full response of the system. In other words, the selected projection vectors in the transformation matrix must be able to approximate any other vector in the space as linear combinations of the mode shape vectors preserved in the reduced space. Figure 3.22 shows the $[U_{12}]$ matrix for the hard contact case using the modes of the configuration with the largest set of active modes needed to preserve the first 5 modes of the system. The red and blue squares show the modes needed to preserve the first 5 modes of the system when no additional modes are active. The green squares show the additional modes used in this case to better approximate the influence of the higher order modes due to the hard contact interactions.

The ADOF selected were 31, 33, 39, 43, 47, 55, 57 and 61 from Beam A, and ADOF 65, 79, 89, 99, 109, 119, 149, 159, 169, 179, 189, 199 and 205 from Beam B. The nonlinear contacts occurred at ADOF 39 and 47 of System 2 like in previous

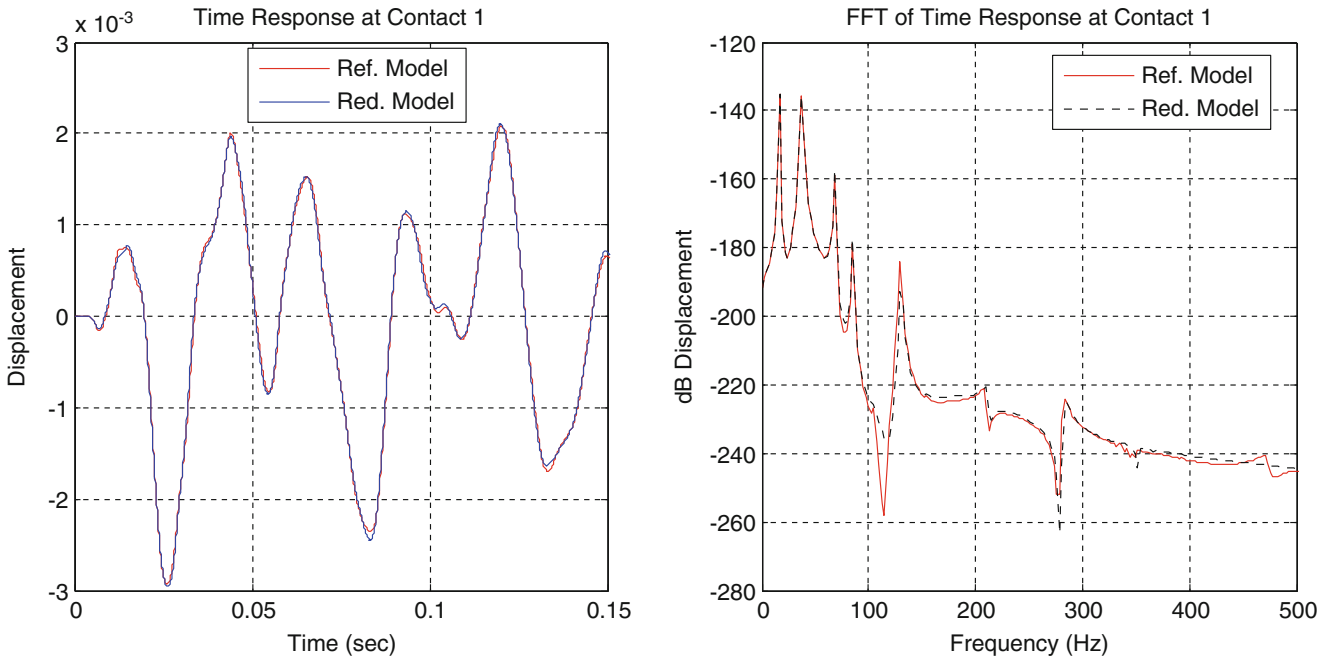

Fig. 3.16 Comparison of response (*left*) and FFT (*right*) of reference and reduced order model at spring contact location 1

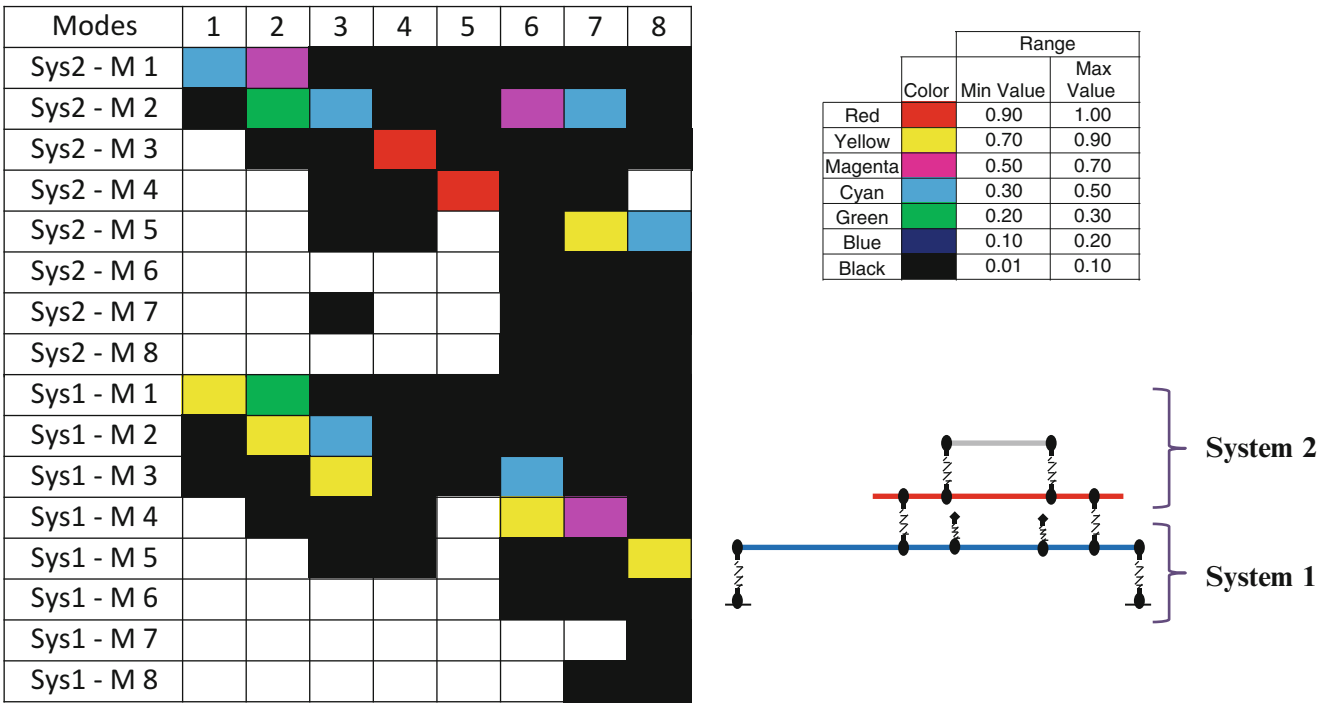

Fig. 3.17 [U_{12}] contribution matrix for model using 8 modes of each System 1 and System 2 for a total of 16 modes

cases. Note that no ADOF are placed at the ancillary subcomponent and/or connecting DOF between the ancillary and Beam A. Figure 3.23 shows the correlation and response for the 21 DOF model and the reference model.

The modes used in the reduced model resulted in an accurate approximation of the response of the NDOF system. However, the effects of mode truncation could not be completely mitigated. Additional modes could have been added, in particular for System 2. However, the 8 modes used and the ADOF selected from System 2 resulted in a more well-conditioned transformation matrix than by randomly adding DOF to the reduced model. The reduced space matrices can

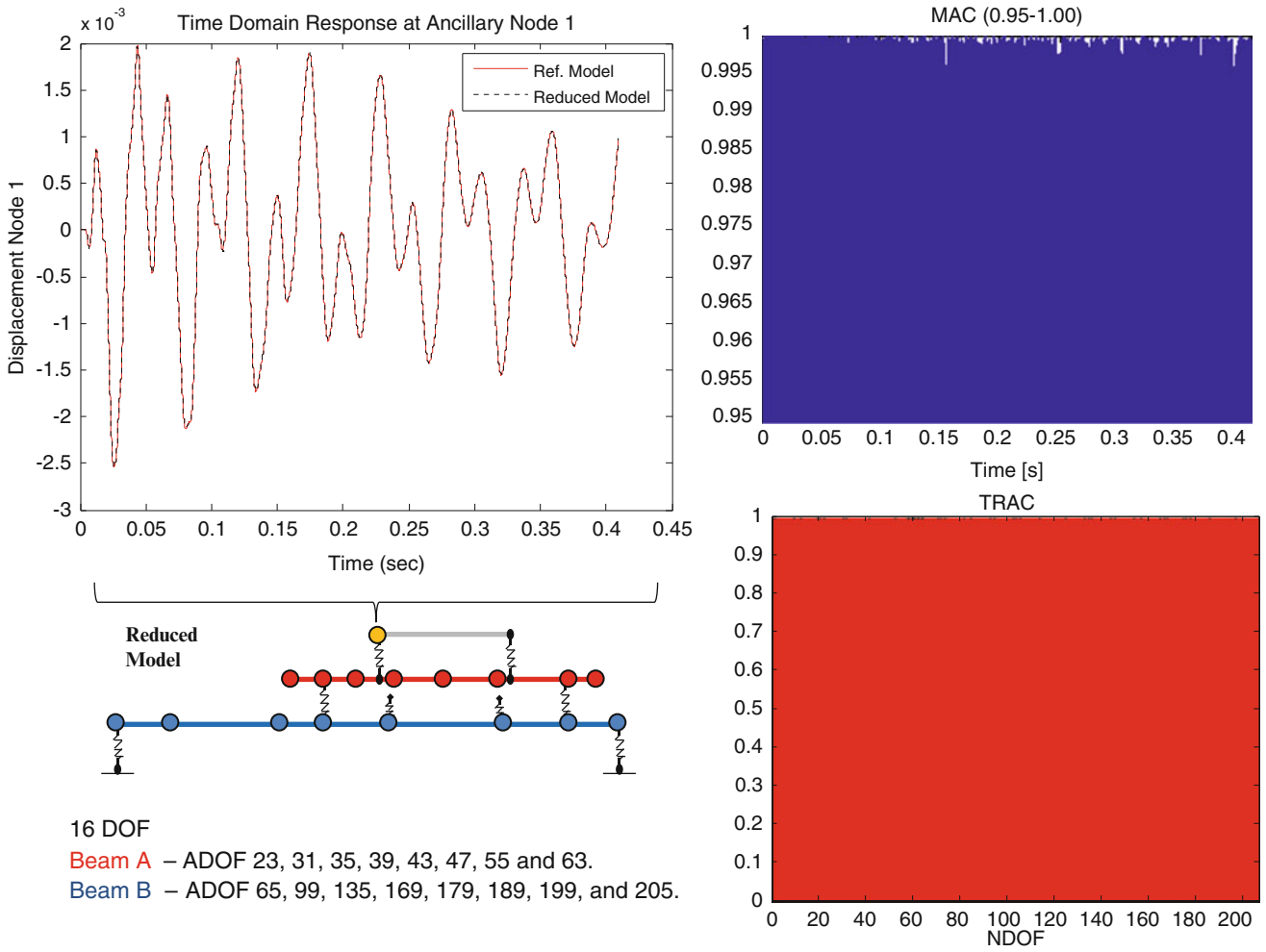

Fig. 3.18 Predicted response at ancillary node 1 from 16 DOF reduced model. MAC from 0.95 to 1.0 (*top right*) and TRAC (*bottom right*) correlation of models

become ill-conditioned for certain choice and number of DOF and the predicted response is then subjected to high levels of numerical error. Nevertheless, Fig. 3.24 shows that the FFT and response at the contact location 1 is reasonably approximated by the reduced model of 21 modes.

The cases considered thus far have shown that full field results can be obtained from reduced order models with subcomponent interactions from the embedded information preserved in the reduction process. Using the necessary number of modes in the reduced model to span the space of all modes of interest allows the response at the ancillary and any other DOF to be predicted accurately. The $[U_{12}]$ contribution matrix and the effect of the higher order modes from nonlinear interactions must be taken into account as well as the linear independence and well-determined behavior of the reduced matrices in order to obtain a good approximation of the dynamic characteristics of the system. Moreover, when proper precautions are taken to reduce the N space system to 'a' space, no ADOF are needed in the dynamically active ancillary subcomponent.

The next set of cases explores the natural extension of this work to include nonlinear contacts occurring at the ancillary subcomponent. For all the reduced models of Case A the nonlinear contact occurred at points that were preserved in the reduction process. This was done in order to check for a change of state in the system due to the springs coming in contact at those locations. However, if the contact were to occur at the ancillary subcomponent the response must be tracked at that location in order to know how the system is changing from one configuration to the other as will be discussed next.

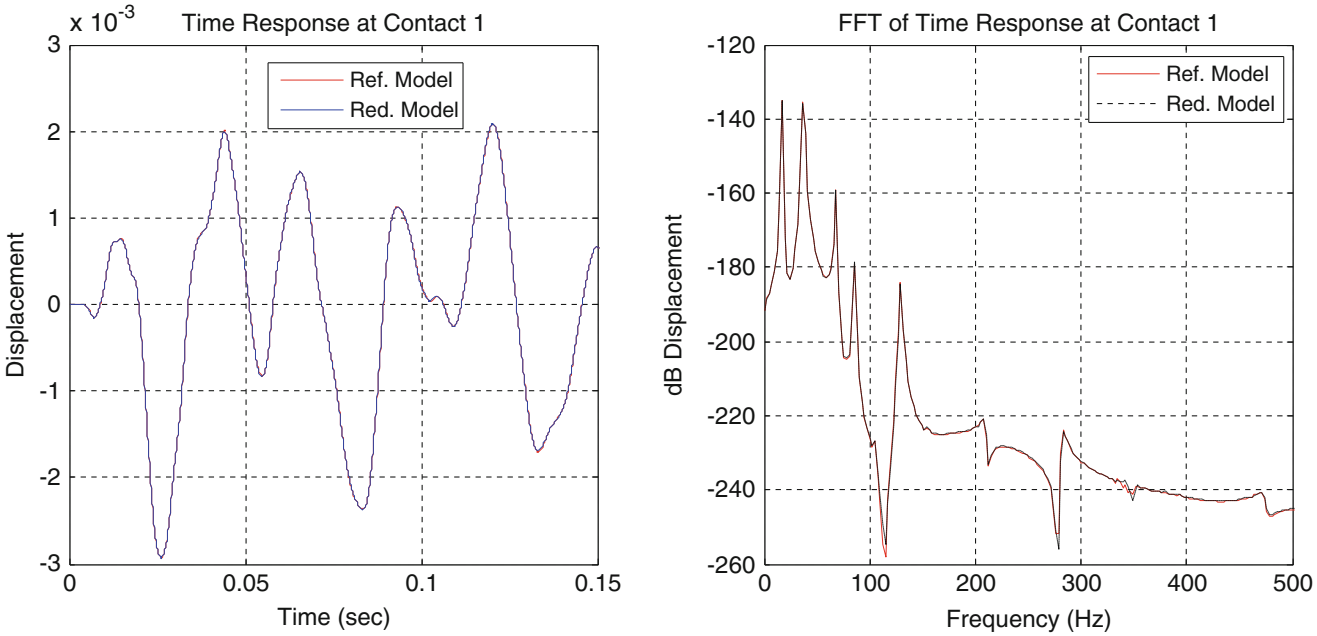

Fig. 3.19 Comparison of response (*left*) and FFT (*right*) of reference and 16 mode reduced order model at spring contact location 1

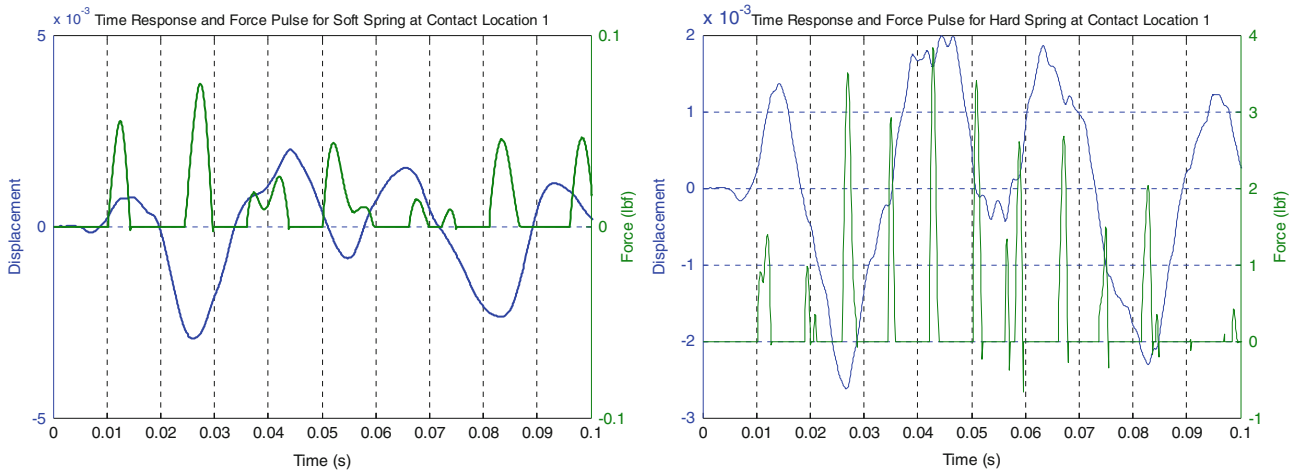

Fig. 3.20 Comparison of soft (*left*) and hard (*right*) type of nonlinear contacts at DOF 37 of the 3 beam system

3.4.2 Case B: One Nonlinear Contact at System 2

3.4.2.1 Case B-1: Soft Contact Reference Solution

The assembled 3 beam structure consisting of System 1 and System 2 (as shown in Fig. 3.1) was constructed with a single nonlinear contact of a 100 lb/in spring. The contact occurs between the ancillary subcomponent (at DOF 11) and Beam A of System 2. The full NDOF (206) response with the new contact configuration (as shown in Fig. 3.10) was calculated for used as a reference with the reduced order models. New $[U_{12}]$ contribution matrices were computed for the two possible configurations of Case B, one when the spring is not in contact and configuration 1 when the spring comes in contact with the ancillary subcomponent. As previously done in Case A, the necessary modes for an accurate prediction of the response were selected from the contribution matrix and with consideration to the higher modes that will be excited due to the hard contact nonlinear connections. Two cases are studied – one with an active DOF at the contact point and one without an active DOF at the contact point; this was studied to determine the effect of location of the active DOF.

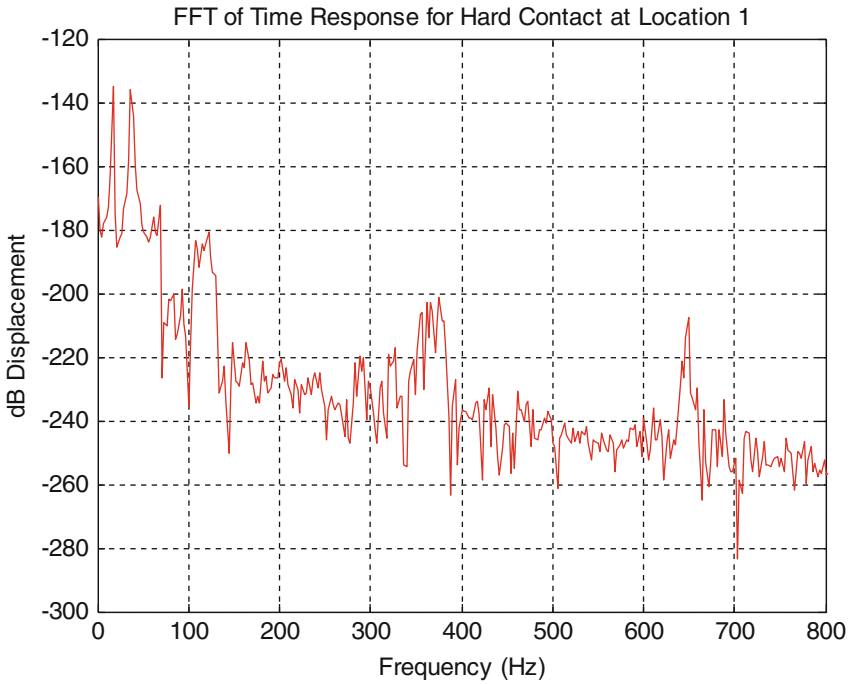

Mode	Frequency (Hz)			
	Conf. 0	Conf. 1	Conf. 2	Conf. 3
1	16.78	16.78	16.78	16.78
2	37.50	37.53	37.52	37.53
3	68.11	68.35	68.25	68.36
4	84.61	98.75	98.86	99.19
5	102.08	125.29	128.83	128.84
6	129.11	144.23	138.43	170.42
7	209.96	215.02	215.85	219.30
8	282.02	282.14	286.27	287.29
9	342.95	380.51	376.62	396.23
10	396.25	396.26	396.47	415.99
11	477.32	478.28	486.09	492.62
12	645.25	679.21	659.51	689.08
13	716.29	717.68	726.23	726.42
14	889.02	889.06	889.04	889.08
15	960.58	960.58	967.53	967.53

Fig. 3.21 FFT of reference NDOF model response at contact location 1 for hard spring (10,000 lb/in) contact

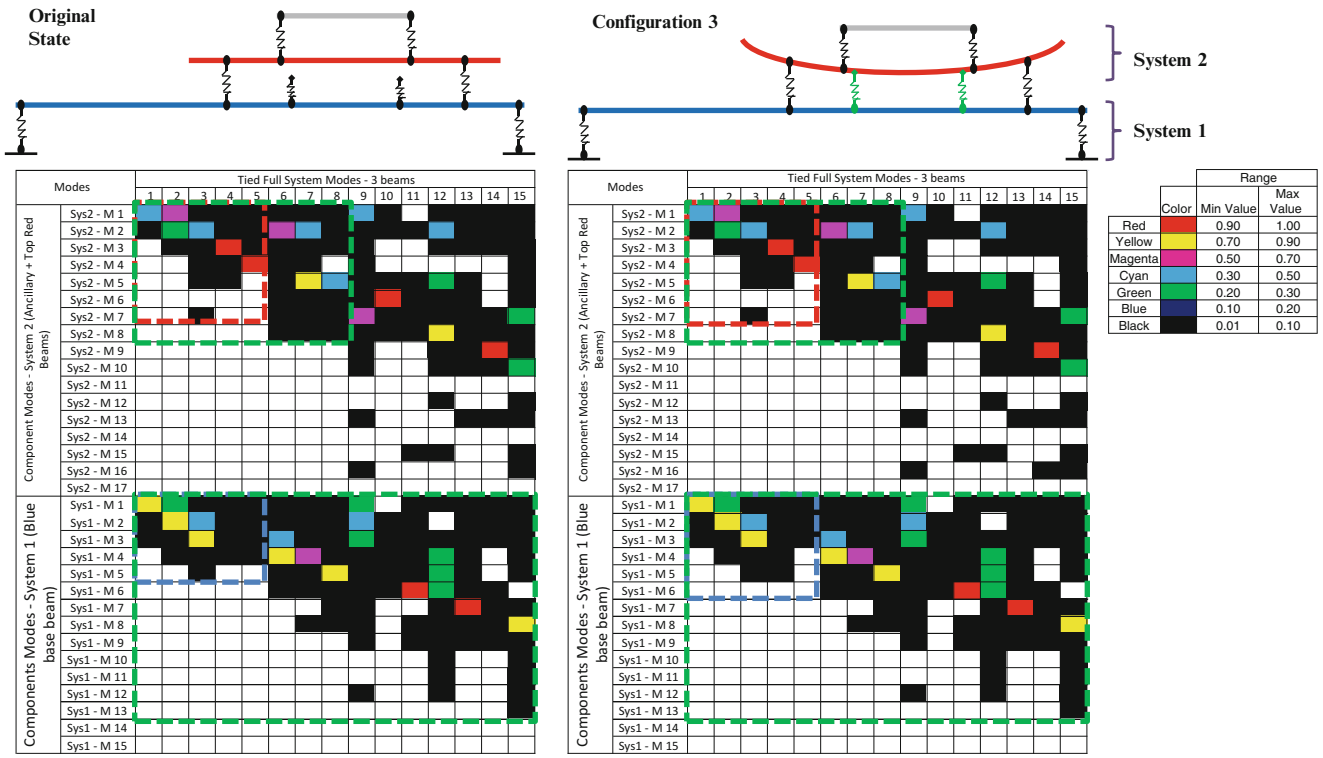

Fig. 3.22 $[U_{12}]$ matrices for configurations 0 and 3 in the hard contact case. *Blue squares* indicate modes needed from System 1, while the *red squares* indicate modes needed from System 2. *Green squares* show additional modes included due to active higher order modes in the response of the system

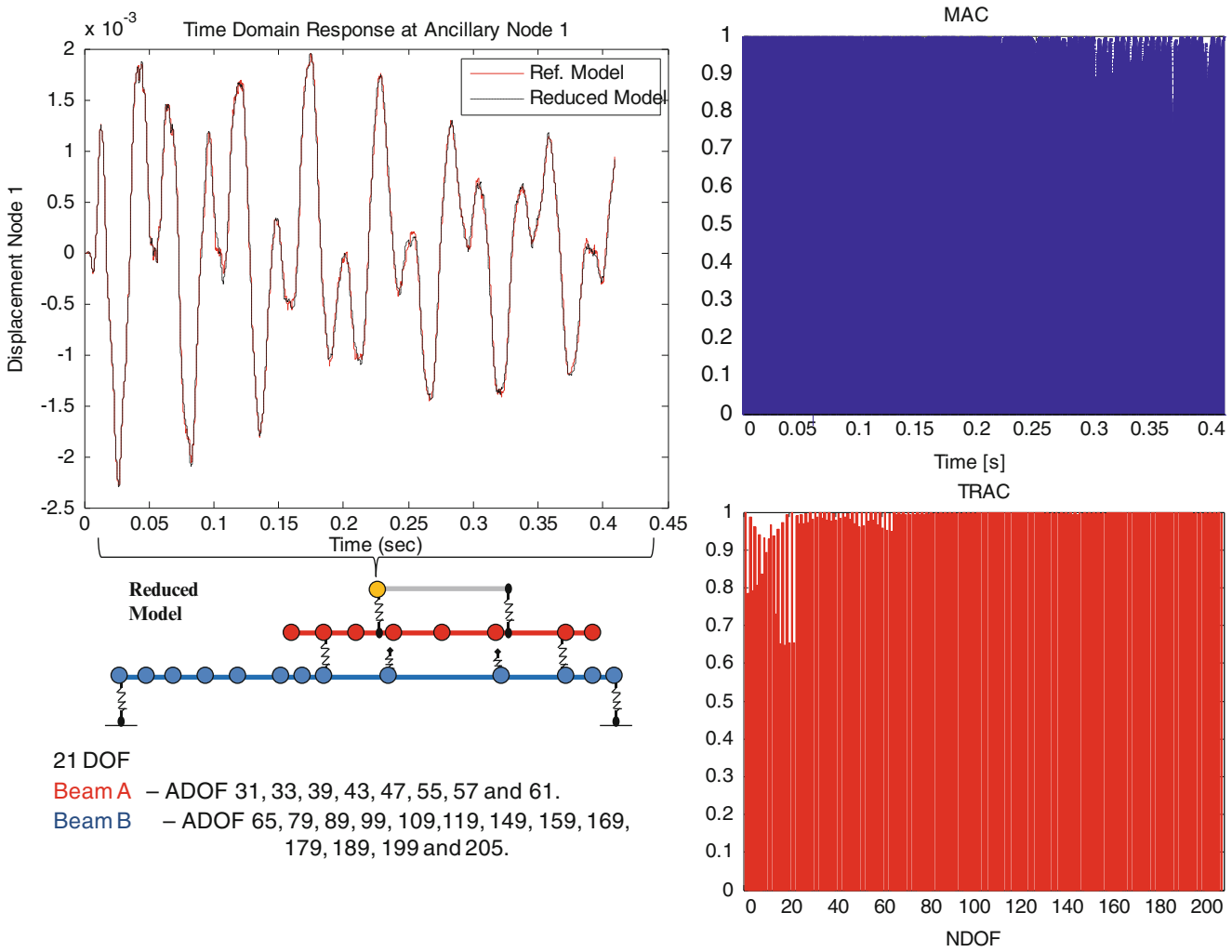

Fig. 3.23 Predicted response at ancillary node 1 from 21 DOF reduced model with hard contacts. MAC (*top right*) and TRAC (*bottom right*) correlation of models

3.4.2.2 Case B-1.1: Soft Contact Reduced Model Solution with 22 Modes with ADOF at Ancillary

A SEREP reduced model of 22 ADOF was computed using modes 1–9 and mode 12, ADOF 65, 97, 117, 137, 157, 169, 177, 185, 199 and 205 from Beam B and modes 1–10, 13 and 16, ADOF 11, 23, 29, 31, 33, 39, 43, 47, 51, 53, 55 and 63 from Beam A. Note that the nonlinear contact of 100 lb/in occurs at Ancillary DOF 11 of System 2 and this point is included in the reduced model. The modes were selected from the $[U_{12}]$ contribution matrix showing the proper number of component modes needed to form the modes of the assembled 3 beam system. Figure 3.25 shows a comparison of the displacement and FFT of the response at the contact location on the ancillary (DOF 11).

Figure 3.26 shows the displacement at node 1 of the ancillary along with the correlation of the reduced model and the reference model. The models showed high levels of correlation at all DOF. However, there are some minor differences that can be observed in the FFT of Fig. 3.25.

The differences can be attributed as in previous cases to the effect of higher order modes. The FFT of the reference model shows active high order modes above 800 Hz which occurs in the vicinity of the 18th mode of the system. Therefore, prediction of the response at all DOF with high accuracy requires modes beyond the 14 modes involved in forming the first 7 modes of the system (those modes active from the input force alone). One of the main objectives of this work is the prediction at the subcomponent level from the embedded component information in the reduction process. The next case will explore whether is possible to compute the dynamic response of the ancillary subcomponent when the nonlinear contact occurs at a DOF not in the reduced model.

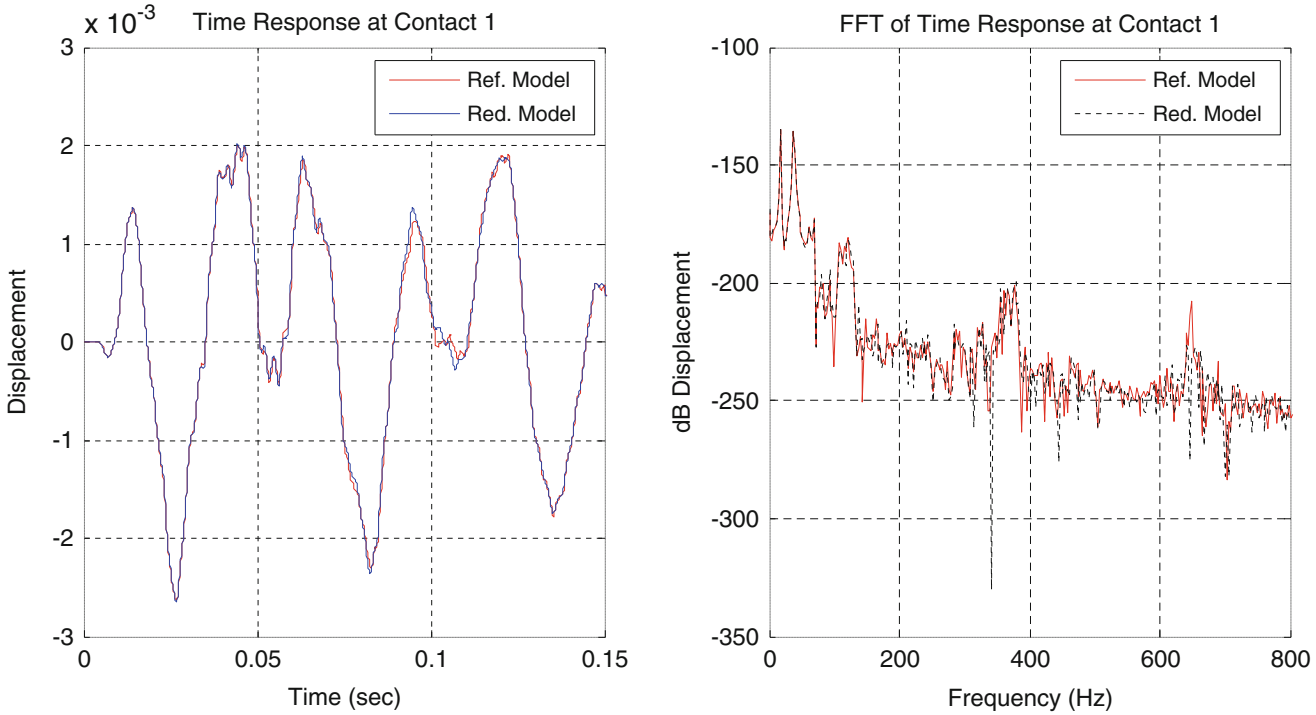

Fig. 3.24 Comparison of response (*left*) and FFT (*right*) of reference and 21 DOF reduced order model at contact location 1

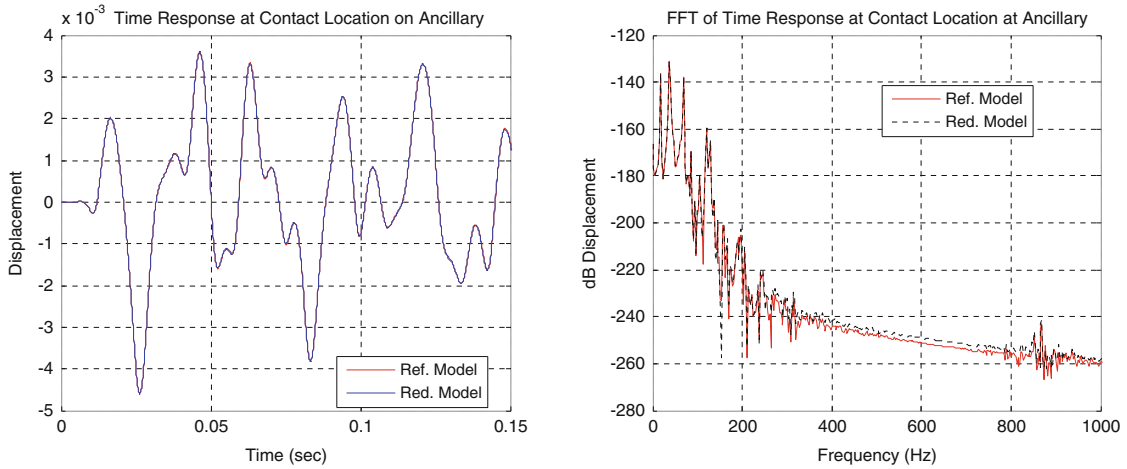

Fig. 3.25 Comparison of response (*left*) and FFT (*right*) of reference and 22 DOF reduced order model at contact location

3.4.2.3 Case B-1.2: Soft Contact Reduced Model Solution with 18 Modes with No ADOF at Ancillary

In a similar manner to that of the previous case, a reduced model of 18 modes was created without the use of an active DOF at point 11 where the nonlinear contact occurs. The reduced model consisted of modes 1–9, ADOF 65, 75, 97, 105, 127, 155, 169, 185, and 199 from Beam B and modes 1–9, ADOF 25, 31, 35, 39, 43, 47, 53, 55 and 61 from Beam A. The nonlinear contact of 100 lb/in was placed at Ancillary DOF 11 of System 2 but no ADOF were selected on the ancillary subcomponent or the connecting DOF between Beam A and the ancillary. In order to check for a change of configuration during the time response of the reduced model, the algorithm used the expansion of the displacement at time t_i for DOF 11 and then continued to the next time step t_{i+1} making the necessary adjustments if the spring came in contact with the ancillary subcomponent. Only the response at DOF 11 was expanded throughout the response since no other DOF are needed during the computation of the reduced model response. The response at 'a' space was expanded to NDOF using the transformation

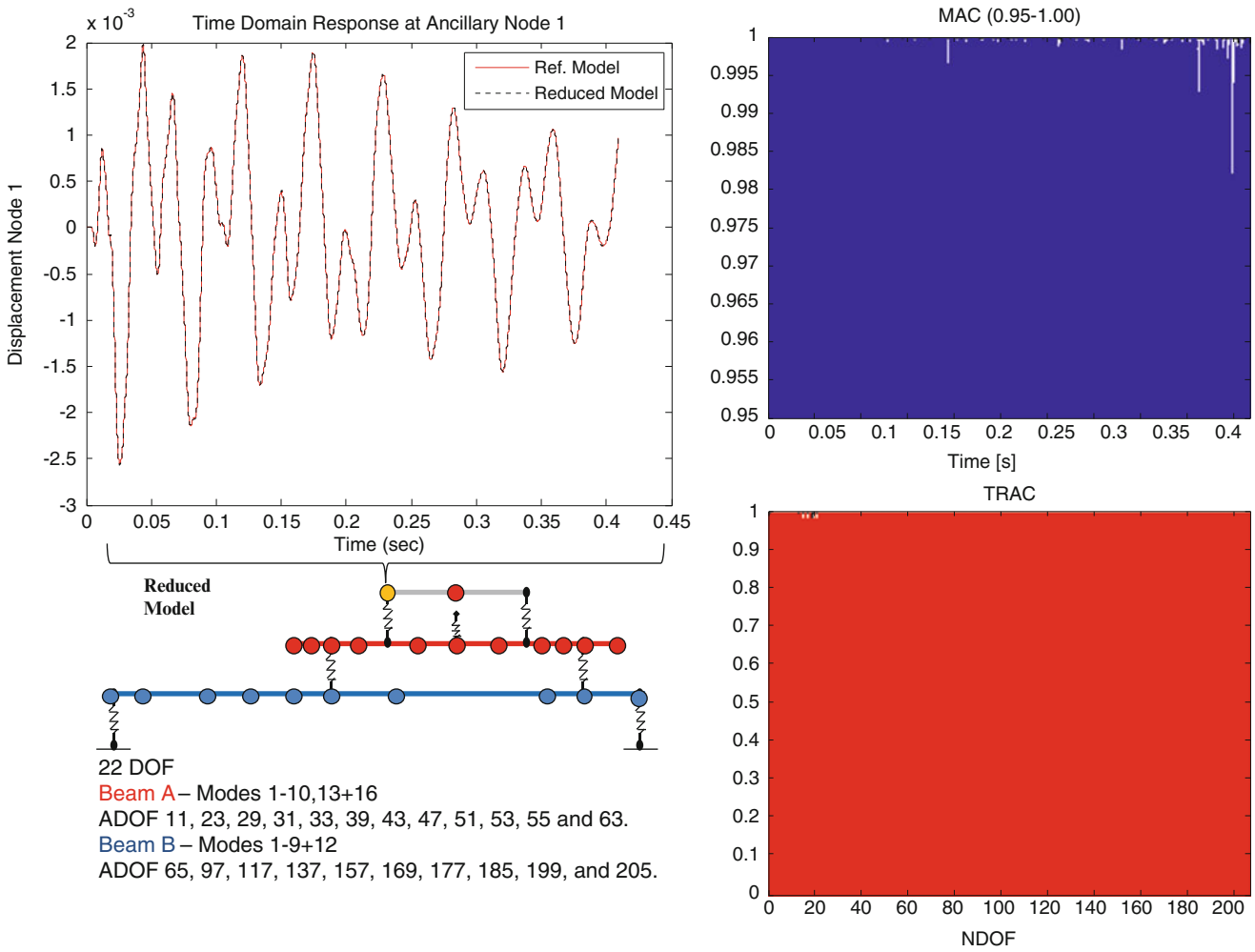

Fig. 3.26 Predicted response at ancillary node 1 from 22 DOF reduced model with soft contact. MAC from 0.95 to 1.0 (*top right*) and TRAC (*bottom right*) correlation of models

matrices (mode shape projection vectors) from the reduction process. Figure 3.27 shows a comparison of the response at point 1 of the ancillary as well as the correlation with the reference model.

The results of this reduced model show that there is an accumulation of error in the predicted system response which may be due to both mode truncation and numerical issues; but additional cases need to be explored before this is more clearly understood. Figure 3.28 shows a comparison of the response and its FFT at the contact location. In the previous case, the contact point was included in the active set of DOF. In this case, the contact point was not included. The results obtained were not as accurate and well behaved as in the previous case. This may be due to many different factors such as numerical issues, rank problems, need for more modes, and many other factors which need to be addressed in future work.

3.5 Conclusions

Nonlinear models of a multiple component structure were created to illustrate the prediction of subcomponent dynamic characteristics from embedded information in the reduction process. Models with multiple and single nonlinear contacts were considering as well as the effect of soft and hard contacts in the response. When enough modes of the unconnected components are preserved such that they form a linearly independent set of vectors spanning the space of the full response, the response was accurately predicted at all DOF of the system. The prediction at the ancillary subcomponent was successfully performed even when no active DOF were preserved in the reduced model. Additional work is needed in order to further

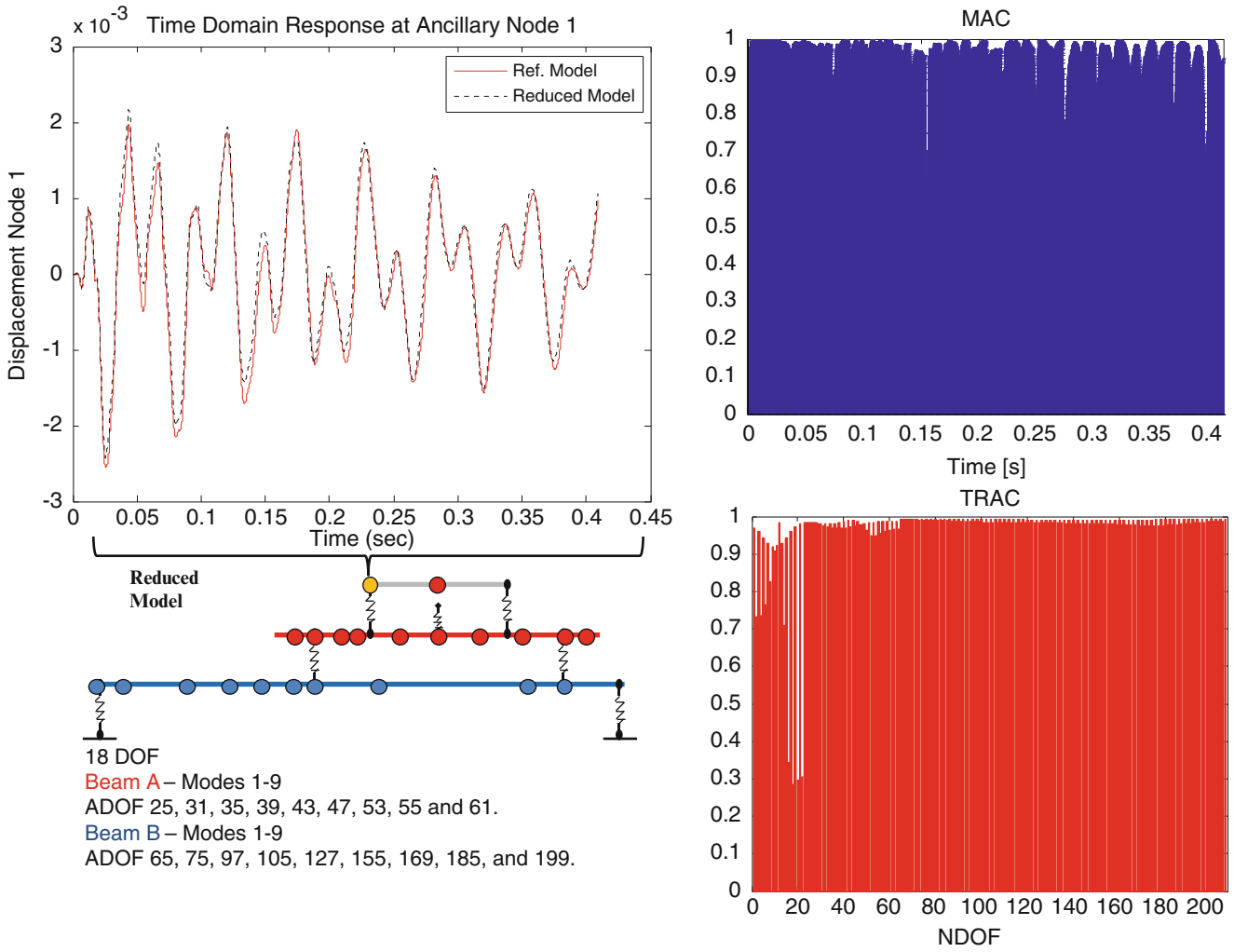

Fig. 3.27 Predicted response at ancillary node 1 from 18 DOF reduced model with soft contact. MAC (*top right*) and TRAC (*bottom right*) correlation of models

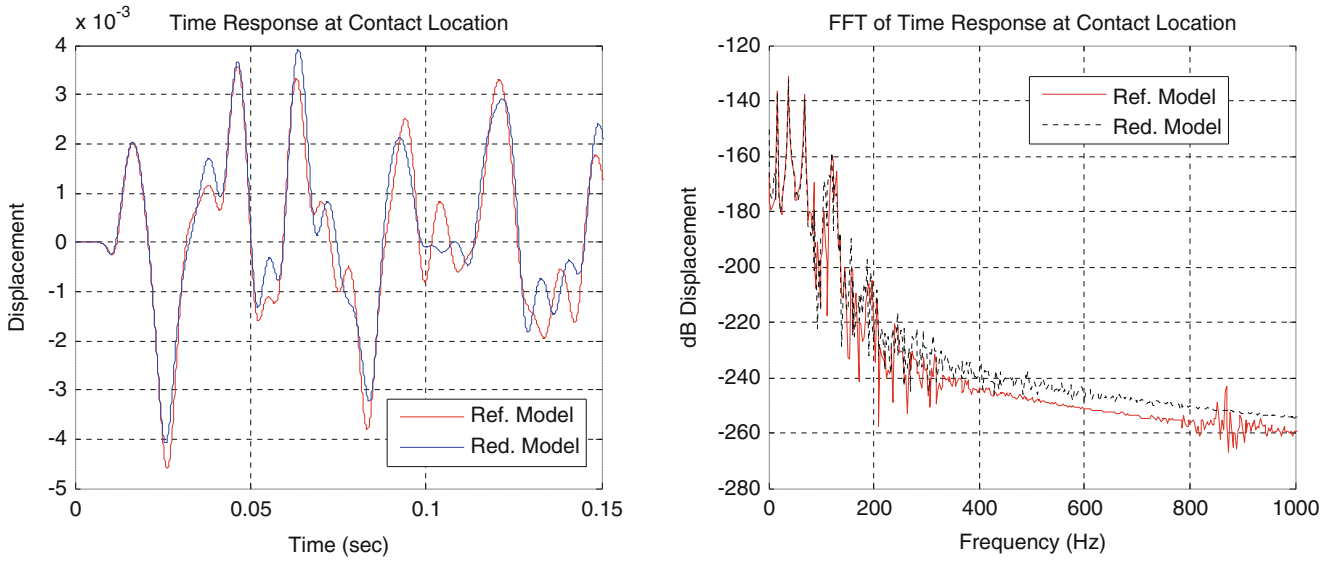

Fig. 3.28 Comparison of response (*left*) and FFT (*right*) of reference and 18 DOF reduced order model at contact location

study the effects of including the contact point as one of the active DOF for the reduced order model. Nevertheless, this work shows significant promise in the prediction of linear and nonlinear subcomponent response in cases where is not possible to place ADOF at the subcomponent level.

Acknowledgements Some of the work presented herein was partially funded by Air Force Research Laboratory Award No. FA8651-10-1-0009 "Development of Dynamic Response Modeling Techniques for Linear Modal Components". Any opinions, findings, and conclusions or recommendations expressed in this material are those of the authors and do not necessarily reflect the views of the particular funding agency. The authors are grateful for the support obtained.

References

1. Thibault L (2012) Development of equivalent reduced model technique for linear modal components interconnected with nonlinear connection elements. Master's thesis, University of Massachusetts Lowell
2. Thibault L, Avitabile P, Foley J, Wolfson J (2013) Equivalent reduced model technique for nonlinear dynamic response. Mech Syst Signal Process 36:422–455. doi:10.1016/j.ymssp.2012.07.013
3. Thibault L, Avitabile P, Foley J, Wolfson J (2012) Equivalent reduced model technique for nonlinear dynamic response. Proceedings of the thirtieth international modal analysis conference, Jacksonville
4. Marinone T, Avitabile P, Foley J, Wolfson J (2012) Efficient computational nonlinear dynamic analysis using modal modification response technique. Mech Syst Signal Process 31:67–93. doi:10.1016/j.ymssp.2012.02.011
5. Marinone T (2012) Efficient computational nonlinear dynamic analysis using modal modification response technique. Master's thesis, University of Massachusetts Lowell
6. Marinone T, Thibault L, Avitabile P (2013) Expansion of nonlinear system response using linear transformation matrices from reduced component model representations. In: Proceedings of the thirty-first international modal analysis conference, Garden Grove
7. Pingle P, Niezrecki C, Avitabile P (2011) Full field numerical stress-strain from dynamic experimental measured data. In: EURODYN 2011, Leuven
8. Avitabile P, Pingle P (2012) Prediction of full field dynamic strain from limited sets of measured data. Shock Vib 19:765–785. doi:10.3233/SAV-2012-0686
9. Pingle P, Avitabile P (2010) Prediction of full field dynamic stress/strain from limited sets of measured data. In: Proceedings of the twenty-eighth international modal analysis conference, Jacksonville
10. Pingle P, Avitabile P (2011) Limited experimental displacement data used for obtaining full-field dynamic stress/strain. In: Proceedings of the twenty-ninth international modal analysis conference, Jacksonville
11. Pingle P, Avitabile P (2011) Full field dynamic stress/strain estimation from limited sets of measured data. In: Proceedings of the twenty-ninth international modal analysis conference, Jacksonville
12. Pingle P (2010) Prediction of full-field dynamic stress/strain from limited sets of measured data. Ph.D. dissertation, University of Massachusetts Lowell
13. Carr J, Baqersad J, Niezrecki C, Avitabile P (2013) Predicting dynamic strain on wind turbine blade using digital image correlation techniques in conjunction with analytical expansion methodologies. In: Proceedings of the thirty-first international modal analysis conference, Garden Grove
14. Carr J, Baqersad J, Niezrecki C, Avitabile P (2012) Dynamic stress–strain on turbine blade using digital image correlation techniques, part 1 – static calibration. In: Proceedings of the thirtieth international modal analysis conference, Jacksonville
15. Carr J, Baqersad J, Niezrecki C, Avitabile P (2012) Dynamic stress–strain on turbine blade using digital image correlation techniques, part 2 – dynamic measurements. In: Proceedings of the thirtieth international modal analysis conference, Jacksonville
16. Carr J (2013) Application of dynamic expansion from limited measurements for full-field stress/strain on wind turbine blades. Master's thesis, University of Massachusetts Lowell
17. Harvie J (2013) Computationally efficient reduced order models for full field nonlinear dynamic strain predictions. Master's thesis, University of Massachusetts Lowell
18. Harvie J, Obando S, Avitabile P (2013) Reduced order system model nonlinear response and expansion for full field results. In: Eleventh international conference on recent advances in structural dynamics, Pisa
19. Avitabile P, Obando SE, Truong K (2014) Full field dynamic deflection and strain for linear components connected with nonlinear connectors. In: Proceedings of ISMA 2014 international conference on noise and vibration engineering, Leuven
20. Avitabile P, Harvie J, Obando SE (2014) Efficient reduced order nonlinear response with expansion for full field results. In: Proceedings of the 9th international conference on structural dynamics, EURODYN 2014, Porto
21. Avitabile P, Nonis C, Obando S (2014) System model modes developed from expansion of uncoupled component dynamic data. Stroj vestn-J Mech Eng 60(5):287–297
22. Nonis C, Thibault L, Marinone T, Avitabile P (2013) Development of full space system model modes from expansion of reduced order component modal information. In: Proceedings of the thirty-first international modal analysis conference, Los Angeles
23. Obando S, Avitabile P (2014) Prediction of forced response on ancillary subsystem components attached to reduced linear systems, vol 1, Dynamics of coupled structures. Springer, Berlin, pp 51–72
24. O'Callahan JC, Avitabile P, Riemer R (1989) System equivalent reduction expansion process. In: Proceedings of the seventh international modal analysis conference, Las Vegas
25. Avitabile P (2003) Twenty years of structural dynamic modification – a review. Sound and Vibration Magazine, pp 14–27
26. Guyan RJ (1965) Reduction of stiffness and mass matrices. AIAA J 3(2):380

27. O'Callahan JC (1989) A procedure for an Improved Reduced System (IRS) model. In: Proceedings of the seventh international modal analysis conference, Las Vegas
28. Obando SE, Avitabile P (2015) Prediction of forced response using expansion of perturbed reduced order models with inexact representation of system modes. In: Proceedings of the thirty-third international modal analysis conference, Orlando (to be published)
29. Newmark NM (1959) A method of computation for structural dynamics. J Eng Mech Div Am Soc Civ Eng 85(3):67–94
30. Chipman C, Avitabile P (2012) Expansion of transient operating data. Mech Syst Signal Process. 10.1016/j.ymssp.2012.04.013. Accepted Apr 2012
31. Chipman C, Avitabile P (2009) Expansion of transient operating data. In: Proceedings of the twenty-seventh international modal analysis conference, Orlando
32. Chipman C, Avitabile P (2008) Expansion of real time operating data for improved visualization. In: Proceedings of the twenty-sixth international modal analysis conference, Orlando
33. Chipman C (2009) Expansion of real time operating data. Master's thesis, University of Massachusetts Lowell
34. Allemang RJ, Brown DL (2007) A correlation coefficient for modal vector analysis. In: Proceedings of the first international modal analysis conference, Orlando
35. Van Zandt T (2006) Development of efficient reduced models for multi-body dynamics simulations of helicopter wing missile configurations. Master's thesis, University of Massachusetts Lowell
36. MAT_SAP/MATRIX (1986) A general linear algebra operation program for matrix analysis, Dr. John O'Callahan, University of Massachusetts Lowell
37. MATLAB R2010a, The MathWorks Inc., Natick